University College London
Department of Electronic & Electrical Engineering

MSc Course Notes
Radar Systems

George Smart
February, 2011

http://www.george-smart.co.uk/

Table of Contents

Introduction

Radar ranging transmits a short pulse of pulse length τ. This then bounces off the target and is received again. From constant velocity formula, we know that the two way propagation delay is:

$\boxed{t = \frac{2r}{c}}$ where t is two way propagation delay, r is the distance to object, and c is the wave-speed.

From this, we rearrange to get the distance of the object, r.

$\boxed{r = \frac{ct}{2}}$ (note, range is sometimes given in nautical miles, 1nmi = 1.85km)

Range Resolution

If we extend our model to two targets, at distances r and $r + \Delta r$, we can find the separation (in time) between the two targets:

$$\boxed{\Delta t = \frac{2(r + \Delta r)}{c} - \frac{2r}{c} = \frac{2\Delta r}{c}}$$

If we adjust our pulse length, τ, to be equal to Δt we can calculate the maximum range resolution for a given pulse length, τ.

$$\boxed{\tau = \Delta t = \frac{2\Delta r}{c}} \quad \rightarrow \quad \boxed{\Delta r = \frac{c\tau}{2}}$$

This means that things closer together than Δr will appear as ones single target. Clearly, from the formula, a shorter pulse length (τ) will give a better range resolution. However, a shorter pulse length also means less energy hits the target, and so targets at a longer range will become invisible due to atmospheric losses – a conflict of interests. Doing some Fourier transforms of square pulses gives a *sinc* function, which we can expect to be the form of the received echo. The bandwidth of this signal at it's 3dB point is

$\boxed{B = \frac{1}{\tau}}$ where B is the signal bandwidth, and τ is the pulse length, as before.

We can then write the range resolution in terms of the bandwidth

$$\boxed{\Delta r = \frac{c}{2B}}$$

Angular Resolution

From antenna theory, we know that the beam-width is related the the physical antenna size,

$\boxed{\Theta_B \approx \frac{\lambda}{d}}$ (λ is the wave-length of the EM signal, d is the physical antenna length)

If we have a range of r, small angle approximation allows us to write that the range resolution would be

$\boxed{r\Theta_B \approx r\frac{\lambda}{d}}$ (for good azimuth resolution, we need a small wave-length or big antenna)

Pulse Repetition Frequency

Radar pulses are transmitted at an interval, known as the pulse repetition interval (PRI). The reciprocal of this gives us the pulse repetition frequency (PRF).

$$PRF = \frac{1}{PRI}$$

Maximum Unambiguous Range

Our pulse repetition interval sets the maximum unambiguous range. This is the maximum range for a target that we can be sure of its position (within the ranges already defined). Consider this scenario: we transmit a pulse to a target at a large range. The two way propagation delay is larger than the pulse repetition interval, and so the echo from the distant target is received by our radar after the transmission of the second pulse. The radar therefore has no idea that the pulse received is a distant echo from pulse one, and not a close echo from pulse two. We can simply define this,

$$r_{unam} = \frac{c \cdot PRI}{2} = \frac{c}{2 \cdot PRF}$$ (note, I have no idea what the symbol used for this is? MUR?)

Scanning Radar

Many radars scan in azimuth (rotate in plane – think airport radar, rotating in circles). If the scan period (time for 1 revolution) is T, then the dwell time for which the beam illuminates the target is

$$t_{dwell} = T \cdot \frac{\Theta_B}{360^\circ}$$ (where Θ_B is in degrees), or $$t_{dwell} = T \cdot \frac{\Theta_B}{2\pi}$$ (with Θ_B in radians)

Hence, the pulses illuminating the target can also be found

$$N_{pulses} = T \cdot \frac{\Theta_B}{360^\circ} \cdot PRF$$

The rotation rate of the antenna in revolutions per minute (rpm) is

$$r.p.m = \frac{60}{T}$$

The Radar Equation

If we have an isotropic antenna (single point, radiating in all directions, equally), then the power density (dubbed Pd) for a square meter of space at distance r from the source can be given as

$$\boxed{Pd = P_t \cdot \frac{1}{4\pi r^2}}$$ (P_t is transmit power, in watts. r is distance between the source and area)

If we change from isotropic antenna to one with a directionality and gain G in the direction of the main lobe, we get the an adjustment of the above formula

$$\boxed{Pd = \frac{P_t G}{4\pi r^2}}$$

The next step is to include the Radar Cross Section area, σ. This is a coefficient of how much energy is reflected back from the target and has units of area. Note, the RCS is not necessarily the same as the objects physical area.

$$\boxed{P_r = \frac{P_t G}{4\pi r^2} \cdot \sigma}$$ (note, we have changed to observe received power, in watts)

We then have the same inverse square distribution of the reflected signal

$$\boxed{Pd = \frac{P_t G}{4\pi r^2} \cdot \sigma \cdot \frac{1}{4\pi r^2}}$$ (note, back to power density again)

We then include the effective antenna area

$$\boxed{P_r = \frac{P_t G}{4\pi r^2} \cdot \sigma \cdot \frac{1}{4\pi r^2} \cdot A_e}$$ (note, we're back to power again, in watts)

The antenna's effective area is related to the gain factor, G, we used before, and the wave-length.

$$\boxed{A_e = \frac{G\lambda^2}{4\pi}}$$ (note, this relates the gain of the antenna to a theoretical area)

We then substitute this in... ...and factorise

$$\boxed{P_r = \frac{P_t G}{4\pi r^2} \cdot \sigma \cdot \frac{1}{4\pi r^2} \cdot \frac{G\lambda^2}{4\pi}} \quad \rightarrow \quad \boxed{P_r = \frac{P_t G^2 \lambda^2 \sigma}{(4\ \pi)^3 r^4}}$$ (the Radar Equation)

Where: P_t = transmitted power, Watts; G = main lobe antenna gain; σ = Radar Cross Section; r = target range; λ = wave-length of EM wave used.

Receiver Noise

The receiver noise power, P_n is given by

$$\boxed{P_n = kT_0BF}$$ (k is Boltzmann's constant, T_0 is the temperature, B is the receiver bandwidth, and F is the receiver's noise figure)

The signal to noise ratio of the Radar system would then be given as

$$\boxed{SNR = \frac{P_r}{P_n} = \frac{P_t G^2 \lambda^2 \sigma}{(4\pi)^3 r^4 k T_0 B F}}$$ (where $T_0 = 290K$ and $k = 1.38 \times 10^{-23}$)

A signal-to-noise ratio of more than $10dB$ would be reasonable for a functioning radar system.

Radar Equation

We also add a loss parameter, L, to accumulate any losses. This include cable loss, sidelobe loss, propagation losses. $0 \leq L \leq 1$.

$$SNR = \frac{P_r}{P_n} = \frac{P_t G^2 \lambda^2 \sigma L}{(4\pi)^3 r^4 k T_0 B F}$$ [minimum SNR to hear target at range r]

Using the above equation, it is possible to calculate the minimum signal-to-noise ratio for given parameters. It could also be rearranged to calculate the maximum detection range for a given set of parameters.

$$r_{max} = \sqrt[4]{\frac{P_t G^2 \lambda^2 \sigma L}{(4\pi)^3 k T_0 B F (SNR)}}$$ (note, 4th root) [maximum range for target detection]

RCS of Flat Plate

The Radar Cross Section of a flat plate of area A is given as

$$\sigma = \frac{4\pi A^2}{\lambda^2}$$ (note the dependence on wave-length used)

Van Atta Arrays

A Van Atta array is a bunch of antennas connected with measured lengths of transmission line. The idea is that the radar signal is received, follows the transmission line, and is re-transmitted in phase, causing a strong radar echo. An n-element Van Atta array has a maximum RCS of (ignoring losses)

$$\sigma_{VA} = \frac{n^2 G_e^2 \lambda^2}{4\pi}$$

RCS of Distributed Targets

The RCS of a given area-distributed target, such as the Earth is given by

$$\sigma = \sigma^0 A$$ (where A is the area of the resolution cell of the radar)

$$A = \frac{c\tau}{2} \times r\Theta_B$$ (range resolution $\times$ angular resolution = area resolution)

σ^0 is dimensionless.

$$\sigma^0 = \frac{\sigma}{A}$$

It will depend on many factors: angle of incidence, dielectric, surface roughness, wave-length, etc.

Integration Gain

All of the above have been in terms of a single pulse. If successive pulses are fired, we can achieve an *integration gain*. For coherent integration (at IF or baseband), the gain is a factor of n. For incoherent integration (after envelope detection), the gain is approximately $n^{0.8}$.

Dynamic Range

The inverse fourth power law means that an echo signal strength varies drastically from short range to long range ($1/r^4$ = 12dB per doubling of range). To cope with this, the gain should be varied through the PRI, from low gain at short range, and high gain at long range. We use either automatic gain control (AGC) or (more usually) sensitivity time control (STC) following the inverse of the inverse-fourth-power law.

Power Aperture Product

Consider surveillance of a solid angle, Ω, with a single beam of solid angle $\omega = 4\pi/G$. The signal-to-noise ratio is

$$\boxed{SNR = \frac{P_r}{P_n} = \frac{P_t G^2 \lambda^2 \sigma L}{(4\pi)^3 r^4 k T_0 B F} \cdot n}$$ [where n is the number of pulses integrated (coherent)]

If the revisit time is T_d, then the dwell time, T_b, is given as

$$\boxed{T_b = T_d \cdot \frac{\omega}{\Omega}}$$

and the number of pulses integrated is $\boxed{n = T_b \cdot PRF}$

The mean transmit power is $\boxed{P_m = P_t \cdot \tau \cdot PRF}$

Hence:

$$\frac{P_r}{P_n} = \frac{P_m}{\tau \cdot PRF} \cdot \frac{4\pi}{\omega} \cdot \frac{4\pi A_e}{\lambda^2} \cdot \frac{\lambda^2 \sigma L}{(4\pi)^3 r^4 k T_0 B F} \cdot T_d \cdot \frac{\omega}{\Omega} \cdot PRF$$

$$\boxed{\frac{P_r}{P_n} = \frac{P_m A_e \sigma T_d L}{4\pi r^4 k T_0 F \Omega}}$$

So we notice that the surveillance performance depends on the product of the mean power, P_m, and antenna aperture area, A_e.

Pattern Propagation Factor

Loss is not the only atmospheric condition to contend with. We also have to consider the Earth's curvature, variation in atmospheric reflective indexes, ground reflections and anomalous propagation (i.e. lift conditions).

Radar Horizon

The Earth's curvature casts a shadow in the area visible to the radar. This means that as the Earth's surface curves away, targets will need to be higher, to be detectable. This is not explained here, as it is basic trigonometry.

Cosec² Antenna Pattern

Suppose an aircraft is flying at height h. As it approaches the radar, it's echo will become stronger according to the $1/r^4$ dependence of the radar equation.

$$\boxed{P_r = \frac{P_t G^2 \lambda^2 \sigma}{(4\pi)^3 r^4}}$$

But, if the vertical-plane pattern of the radar antenna is such that

$$G = G_0 \cdot \frac{r^2}{h^2} = G_0 cosec^2(\theta)$$

Then...

$$P_r = \frac{P_t G_0^2 \lambda^2 \sigma \cdot cosec^4(\theta)}{(4\pi)^3 r^4}$$

$\rightarrow$ ...which cancels to...

$$P_r = \frac{P_t G_0^2 \lambda^2 \sigma}{(4\pi)^3 h^4}$$

… which doesn't depend on range.

Noise, Clutter & Detection

Noise

If we assume that the noise was random, and such that both the I and Q components of the noise had a zero-mean Gaussian (normal) probability distribution function (pdf), we can verify that the central limit theorem is valid. The amplitude of the noise follows a Rayleigh distribution, with the power following (as measured by a square-law detector) would be a negative exponential.

Detection

So detection is a statistical process. If we set a detection threshold, V_T, then there is finite probability of false alarm on noise alone:

$$P_{FA} = \int_{V_T}^{\infty} p_n(R)_{noise\ alone} \cdot dR$$

and there will also be a finite probability of detection with a target present:

$$P_d = \int_{V_T}^{\infty} p_s(R)_{target+noise} \cdot dR$$

[some content missing, assumed not relevant – see original notes]

The signal-to-rms-noise voltage ratio is related to the signal-to-noise power by

$$\frac{A}{\Psi_0} = \frac{signal\ amplitude}{rms\ noise\ voltage} = \sqrt{\frac{2S}{N}}$$

From this, we can plot curves for detection probability vs signal-to-noise ratio for given probability of false alarm.

Target Echo Fluctuation & Swerling Models

So far we have assumed that the target is made from one big component and that it has a constant RCS. However, this may not be the case. Often, the RCS changes from scan to scan (think people walking on ship's deck), or even from pulse to pulse (think Helicopter rotors). Peter Swerling studied this, and crated some models.

Model	Composition	Pulse to Pulse	Scan to Scan
Swirling 0	One dominant	Correlated	Correlated
Swirling 1	Many similar	Correlated	Uncorrelated

Swirling 2	scatterers	Uncorrelated	Uncorrelated
Swirling 3	One dominant, few smaller scatterers	Correlated	Uncorrelated
Swirling 4		Uncorrelated	Uncorrelated

Clutter & Clutter Models

Thus far, our consideration has only been in terms of surface backscatter coefficient, σ^0, which can be used with the radar equation to calculate the clutter power, and hence signal-to-clutter ratio. But the clutter is made from many scatterers within the radar's resolution cell, so the clutter itself is a noise process. You can therefore see the necessity to understand the nature of clutter and the statistics to accurately predict the radar's detection performance. Real clutter distributions are a function of surface type (land, sea, etc), radar frequency, radar resolution, angle of incidence, polarisation, angle of radar 'look', etc. Various clutter models exist, such as the Rayleigh, Ricean, log-normal, Weibull and compound-K models.

Constant False Alarm Rate (CFAR) Processor

CFAR is a common form of adaptive algorithm to detect targets in amongst noise and clutter. It's role is to determine the power threshold above which a signal can be considered to originate from a target. If this threshold is too low, more targets will be detected at the expense of increased false alarms. Conversely, if the threshold is too high, fewer targets will be detected, and the false alarms count will be low. In most systems, the threshold is set in order to achieve a required probability of false alarm. If the background noise is constant with time and space, then a fixed threshold level can be chosen that provides a specified probability of false alarm. In most systems, unwanted clutter and interference noises change both spatially and temporally. In this case, a changing threshold can be used to maintain a constant probability of false alarm.

In simple CFAR schemes, the threshold level is calculated by estimating the noise floor around the cell under test (CUT) by taking a block of cells around CUT and calculating the average power level. To avoid corrupting this estimate with power from the CUT itself, cells immediately adjacent to the CUT are normally ignored ("guard cells"). A target is declared present in the CUT if it is both greater than all its adjacent cells and greater than the local average power level. The estimate of the local power level may sometimes be increased slightly to allow for the limited sample size. This simple approach is called a cell-averaging CFAR (CA-CFAR).

CFAR detectors have several problems:

Self Masking	Bigger objects push up the average around the CUT, casing it to mask
Mutual Masking	Several targets push up the average so none of them are detected.
Edge Performance	-

Some improved schemes have been proposed and evaluated:

Cell-Averaging Greater Of	Attempts to overcome self masking
Ordered Statistic	Mutual Masking
Trimmed Mean	-
Censored Mean	-

A CA-CFAR system will not be able to estimate the clutter exactly, due to the finite sample length. The estimate of mean clutter level will have a distribution of its own, giving a fluctuating value instead of a fixed value – this causes an increased threshold than is ideal, resulting in a higher required SNR, the difference of which is defined as CFAR loss. CFAR loss is also observed as an

increase in threshold value multiplier to achieve a desired PFA – this will be very close to the CFAR loss.

Displays

Various types of display exist. The IEEE Standard 686-2008 defines these.

Scope Type	Description
A-Scope	Oscilloscope display. Range/time on X; Echo amplitude on Y.
B-Scope	Range on Y; Bearing on X; Intensity on Z.
PPI	Plan Position Indicator. Radar in centre; Bearing around as angle; Intensity on Z.
RHI	Range Height Indicator. Range on X; Altitude on Y; Intensity on Z.

Modern aircraft radar have a Track Data Block (TDB) which, using SSR, can give the aircraft callsign, flight levels, ground-speeds and routes. Modern ATC terminals can alert the operator if it predicts a conflict, etc.

Doppler and MTI

In many radar applications, there is a relative movement between between the radar and the target. Examples include air traffic control (ATC), battlefield surveillance, weapon locating, airborne radar, SAR and ISAR as well as many others. Consider ATC. It has to detect incoming and outgoing aircraft in the presence of background clutter. We have already seen that clutter can be distinguished from receiver noise by virtue of it's narrower, low frequency spectrum. A processor that can distinguish moving targets from clutter by virtue of movement is called a moving target indicator (MTI). MTI processors can have many forms.

The Doppler Effect

The phase represented by the two-way path from radar to target and back is

$$\boxed{\phi = 2\pi\frac{2r}{\lambda}}$$

The Doppler shift is

$$\boxed{f_D = -\frac{1}{2\pi}\frac{d\phi}{dt}}$$ (note, the – is due to phase lag as target moves away from radar)

$$\boxed{f_D = -\frac{1}{2\pi}\frac{d}{dt}\left(\frac{4\pi r}{\lambda}\right) = -\frac{2}{\lambda}\frac{dr}{dt} = -\frac{2vf_0}{c}}$$ (note, $+v$ is going away from radar)

Delay Line Canceller

An MTI system attempts to maximise signal-to-clutter ratio (SCR) and are therefore reliant on the correlation of clutter. The Delay Line MTI calculates the difference between the current and previous echo. For moving targets, the echoes will change from pulse to pulse, so the MTI output will be non-zero. Echoes from stationary clutter will be identical, and therefore are suppressed. MTI systems can use phase, amplitude or both to improve the SCR. Systems that use either amplitude or phase do not match the performance of systems using both. Virtually all modern systems use quadrature channel processing (both). The delay line is typically 1 PRI delay, followed by a subtracter to which both the current echo and delayed echo are fed into. The output signal is then processed as normal. The frequency response of a delay line filter is

$$\boxed{|H(\omega)| = 2\left|\sin\left(\frac{\omega T}{2}\right)\right|}$$

Blind Speeds

Plotting this frequency response reveals that the filter has zeroes at Doppler shifts corresponding to

$$\boxed{f_D = \frac{n}{PRI} = n \cdot PRF}$$ (note, n here is an integer, and nothing to do with pulse numbers)

This means, therefore, that at these Doppler shifts, the radar system is unable to detect the presence of a target. In terms of velocity, this gives

$$\boxed{v_{blind} = \frac{n \cdot \frac{\lambda}{2}}{PRI} = \frac{n \cdot c \cdot PRF}{2f_0}}$$

This also tells us that to keep the the first blind speed above the highest likely target velocity it is necessary to use a *high* PRF. This conflicts with the requirement to use a low PRF to avoid range

ambiguity. This is an example of the trade-offs involved with radar design. This is covered in more detail when considering the ambiguity function.

Also note that a target moving tangentially to the radar will have no Doppler, and hence will not be noticed by the MTI.

Cascaded MTI Filter

Often, clutter has a finite spectrum and a variable Doppler spectrum (the sea, blowing trees). Thus the two-pulse canceller does not achieve enough clutter suppression. For improved performance, two delay line cancellers may be cascaded. This is known as the cascaded MTI filter. The frequency response is the square of the single element filter.

$$\boxed{|H(\omega)| = \left(2\left|\sin\left(\frac{\omega T}{2}\right)\right|\right)^2 = 4\left|\sin^2\left(\frac{\omega T}{2}\right)\right|}$$

Plotting the graph of this frequency response, we see that we get better suppression close to zero Doppler.

Staggered PRFs

To address the problem of blind-speeds, it is possible to use a staggered PFR. In this, we relate the two PRFs by an integer ratio $n : m$. We send a pulse, wait for T_1, then send a pulse, wait for T_2, send another pulse, and the process continues. If for example we use a ratio of $4 : 5$, we notice that the first blind speed has been moved to $4/T_1 = 5/T_2$.

Clutter Locking

The presence of a mean clutter velocity can really screw up the effect of the MTI. This mean velocity can originate from the average motion of the clutter or from movement of the radar platform (i.e. on an aircraft). Clutter Locking is a method for removing this average clutter frequency/velocity.

The average interpulse phase is measured and averaged over several range bins. This provides an estimate of the average clutter velocity. This average velocity may then be used to compensate in the delay line circuit. Clearly this will not work if the clutter has a range of velocities, or if the clutter velocity is similar to the target's.

MTI Improvement Factor

MTI performance is measured in two quantities: Clutter Attenuation (CA) and System Improvement Factor (I).

Clutter Attenuation is defined as the clutter power and the input divided by that at the output.

$$\boxed{CA = \frac{input\ clutter}{output\ clutter} = \frac{C_i}{C_o}}$$

System Improvement Factor is defined as SCR at the output, to that at the input.

$$\boxed{I = \frac{\bar{S}_o/C_o}{\bar{S}_i/C_i} = \frac{\bar{S}_o}{\bar{S}_i} \cdot CA}$$

Moving Target Detection

Moving Target Detection (MTD) is an improvement on the simpler MTI. Consider the cascaded MTI system as an N point FFT performed on a time sequence of range bins. The zero Doppler bin is removed prior to processing. We know that not all clutter falls into the zero Doppler bin, and that some targets can have inconsistent Doppler histories. An MTD allows full advantage to be taken in both he Doppler and range domains. A 'clutter map' can be formed in range-Doppler space that is time averaged representation of the clutter in each range bin. MTD is a form of pulse Doppler processing, described later.

Displaced Phase Centre Antenna

Consider an antenna carried on an aircraft and looking out sideways to the direction of travel. The clutter collected will have a velocity component due to the finite beam-width of the antenna and the forward motion of the aircraft. This will mask slow moving targets. One way to improve this is to use two antennas in such a way that antenna two moves to the position of antenna one on subsequent pulses. Thus it can be seen that the 'scene' is viewed from the same antenna position, although it is not the same antenna. This is known as 'arresting' the forward motion. Subtraction of the two signals will remove stationary clutter and reveal moving targets. A third antenna may be added to create a 'monopulse' system to improve angular accuracy. This is used in the US JSTARS system.

Adaptive Doppler Filtering

The Doppler spectrum of clutter can be quite variable, depending on the type of surface (land, vegetation, urban, sea) and also the weather conditions. To properly suppress clutter, and adaptive filter is necessary. The theory is exactly the same as that for an adaptive antenna array. We show later that the covariance matrix of a set of pulses can be used.

$$\hat{\mathbf{W}} = k\mathbf{C}^{-1}\mathbf{D_0}$$

Sideways-Looking Airborne Radar

The Doppler shift of echoes from stationary targets is a function of an off-boresight angle, θ.

Doppler Shift:

$$f_D = \frac{2vf_0\sin(\theta)}{c}$$

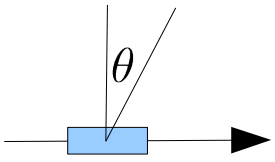

So Doppler shift is 0 for targets at boresight, positive for targets ahead of boresight and negative for those behind.

Space Time Adaptive Process

The figure shows a two-dimensional plot of clutter and jamming, as a function of angle ($\sin(\theta)$, extending from -1 to +1) and Doppler (extending from $-PRF/2$ to $+PRF/2$). There is a weak signal at boresight, and you can appreciate that 2-D filtering is required to suppress both the clutter and jamming to resolve the target.

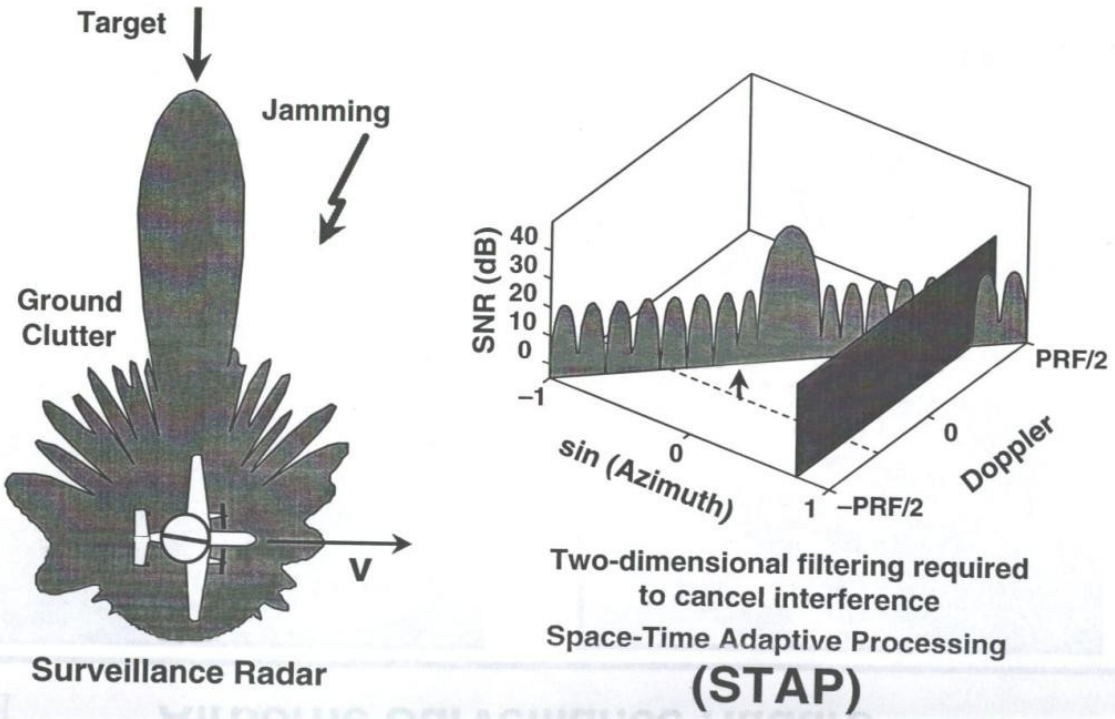

This STAP cube is used to estimate the covariance matrix. A hot topic of research is to find computationally simple ways to get the inverse covariance matrix, as direct inversion is not practical.

The formula below can be used to estimate the Space-Time Covariance Matrix:

$$\hat{R} = \frac{1}{K}\sum_{k=1}^{K} Y_k Y_k^H$$

Problems in calculating this are similar to those encountered with the calculation of the CFAR threshold value. There are several approaches to work around this. One approach uses terrain information to select the appropriate STAP algorithm.

Pulse Compression

Starting with the standard radar equation

$$\boxed{\frac{P_r}{P_n} = \frac{P_t G^2 \lambda^2 \sigma L}{(4\pi)^3 r^4 k T_0 B F}}$$

For a simple pulsed radar system, bandwidth B would be matched to the pulse length, τ, such that $B \approx 1/\tau$ and so

$$\boxed{\frac{P_r}{P_n} = \frac{P_t \tau G^2 \lambda^2 \sigma L}{(4\pi)^3 r^4 k T_0 F}}$$

The product $P_t\tau$ represents the energy of the transmitted pulse. High range resolution demands a short value of τ but good detection range demands for a high transmit energy, and as such, a high value of τ. So instead of sending a short pulse, we send a long pulse modulated in some way as to spread the energy over a bandwidth B to give the required range resolution (i.e. $\Delta r = c/2B$).

The energy of the transmitted pulse is now $P_t\tau$ so the radar signal-to-noise radio for a given target at a given range has been increased by the factor $\boxed{T/\tau}$ or $\boxed{BT}$. This is the *time-bandwidth product* and is also the *processing gain* provided by the pulse compression processing. It is often given in dB, as $\boxed{10\log_{10}(BT)}$.

The maximum detection range for a given target will increase by the 4th-root of the processing gain, so, a factor of $\boxed{\sqrt[4]{BT}}$.

Matched Filter

A good radar system wishes to maximise the peak signal power to mean noise power at the output. Using Fourier transforms to analyse the power spectrum of the signals and noise, and Schwarz's inequality, it is possible to calculate transfer functions for the receiver which maximise the peak signal power:

$\boxed{H(\omega) = KF^*(\omega)e^{-j\omega t_0}}$ (K is constant gain, and t_0 is the time delay though the filter)

This says that the frequency response of the matched filter is equal (aside the gains K and t_0) to the complex conjugate of the signal spectrum, $F(\omega)$.

In the time domain, the impulse response of the matched filter is a time-delayed inverse of the input waveform multiplied by a simple gain constant.

$\boxed{h(t) = K_2 \cdot u^*(t_0 - t)}$ (K_2 is another constant gain, and t_0 the time delay through the filter)

The time-domain output is the convolution of the input signal with the impulse response. This is the autocorrelation function of the input signal (in the absence of noise).

In summary:

- The matched filter maximises the ratio of peak signal power to mean noise power.
- The frequency response is the complex conjugate of the spectrum of the input signal.
- The matched filtered output waveform is the autocorrelation function of the input waveform.

Linear FM

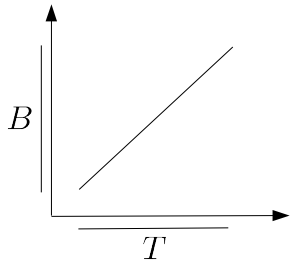

One of the simplest and most widely-used form of modulation used to spread the bandwidth of a long transmitted pulse is the linear frequency modulated *chirp*.

$$u(t) = \cos\left(\omega_0 t + \frac{\mu t^2}{2}\right) \quad \text{where} \quad \mu = \frac{2\pi B}{T}$$

The spectrum of linear FM is given by Fourier transform, and is not included here. See *Klauder et al, 1960* for details. As the time-bandwidth product increases the spectrum approaches a rectangular shape of bandwidth B.

The autocorrelation function of the linear FM signal can be calculated by convolution, but is not included here. The important thing to note is that it has the characteristic $sin(x)/x$ form with a peak sidelobe level of $-13.2dB$.

Surface Acoustic Wave (SAW) Dispersive Delay Lines

SAW technology has been developed to generate and compress waveforms. They consist of piezoelectric transducers at the input and output to convert the electrical signal in to an acoustic signal (mechanical vibration) which propagates as a surface acoustic wave. Various geometries are available; the reflective compressive array uses etched lines on the surface at several intervals of varying spacing which act as resonant reflectors when the spacing is equal to the surface wave frequency. In this way, the device acts as as a dispersive delay line (i.e. that the time delay is a function of frequency) since different frequencies encounter different path lengths. Hence the frequency components of a short pulse will disperse to generate a chirp signal. The inverse characteristic can be used to compress the echo in the receiver. Amplitude weighting can be added to reduce range sidelobes.

Advantages and Disadvantages of Pulse Compression

- **Advantages**
  - More efficient use of average power available at radar. In some cases, avoidance of peak-power problems in the high power sections of the transmitter
  - Increased system resolving capabilities in both range and velocity. In case of range resolution, the need to generate extremely fast rise-time, high power signals is avoided by using pulse compression.
  - Reduced vulnerability to certain types of interfering signals, for example those which do not have the same properties as the coded waveform.
- **Disadvantages**
  - Increased minimum range due to longer pulses preventing reception of short range echoes. This is not usually a problem, as parameters can be tweaked to overcome the problems for a given situation.
  - Range sidelobes. These are a problem.

The Ambiguity Function

We have seen that the output of a matched filter for a given waveform as a function of time (the *point target response*) is given by the autocorrelation function of that waveform:

$$g(t) = \int u(t) \cdot u^*(x-t)dx$$

Woodward generalised this idea to consider the response of a matched filter for a given waveform to an echo and associated a Doppler shift. The Ambiguity function is defined as:

$$\left|\chi(\tau, v)\right|^2 = \left|\int u(t)u^*(t+\tau)e^{j2\pi vt}dt\right|^2$$

If the signal amplitude is normalised such that $\int \left|u(t)\right|^2 dt = 1$, then we notice that $\iint \left|\chi(\tau, v)\right|^2 d\tau dv = 1$. This is an important result as it tells us that energy suppressed in the ambiguity function must reappear somewhere else.

Range Sidelobes

Range sidelobes, also referred to as time sidelobes, of echoes from strong targets can obscure weaker, closer targets in the same way as antenna sidelobes – but range sidelobes do not have the two-way protection of the antenna sidelobes. They can be reduced using an amplitude taper. The same taper functions as antenna sidelobe reduction can be used, and have the same effects of loss and broadening of the main sidelobe.

Ambiguity Diagram

This is a powerful and intuitively appealing way of representing the performance of a given waveform. A 3-D plot of the ambiguity function is referred to as the *ambiguity diagram*. X-axis shows Doppler (velocity), the Y-axis shows time (range), and the Z-axis shows $\left|\chi(\tau, v)\right|^2$ (ambiguity). It contains a large amount of data, including range and Doppler resolution, sidelobe level and ambiguity spacing (blind speeds).

Monostatic Ambiguity Function

Central peak gives an estimate of range resolution (ability to distinguish between multiple targets) and Doppler resolution (clutter rejection). Appearance of other peaks in the range-Doppler plane correspond to potential ambiguities.

Matched Filtering:

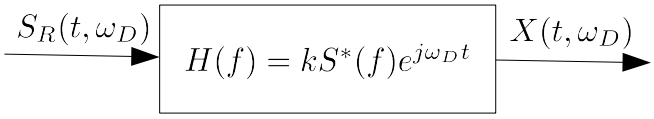

Formula:

$$X(t, \omega_D) = \int_{-\infty}^{\infty} u(t)u^*(T-t)e^{j\omega_D t}dt$$

Range-Doppler Coupling

The ambiguity function of linear FM has a diagonal ridge, caused by range-Doppler coupling. This is because the echo that is shifted by a Doppler frequency f_D will almost correctly be filtered by the matched filter to a zero-Doppler echo but with a range error

$$\boxed{r_{err} = f_D \times \frac{T}{B}}$$

This is known as range-Doppler coupling, and also occurs in FM radar.

Effect of Phase and Amplitude Errors

Phase and amplitude errors introduced by a practical radar system will have the effect of degrading the range sidelobe level (point target response). Can use the *actual* transmitted pulse as a range reference function.

Waveform Design

Barker Codes

Barker codes are a set of binary (biphase) codes with perfect autocorrelation properties in the sense that the sidelobes are either -1, 0 or +1. The codes are as follows:

Code Length	Code Elements	Sidelobe Level, dB
2	$+-$ OR $++$	$20\log_{10}(02) = -6.0$
3	$++-$	$20\log_{10}(03) = -9.5$
4	$++-+$ OR $+++-$	$20\log_{10}(04) = -12.0$
5	$+++-+$	$20\log_{10}(05) = -14.0$
7	$+++--+-$	$20\log_{10}(07) = -16.9$
11	$+++---+--+-$	$20\log_{10}(11) = -20.8$
13	$+++++--++-+-+$	$20\log_{10}(13) = -22.3$

We evaluate the autocorrelation function for any of these codes by considering the output for a tapped delay-line matched-filter. For a code length, n we notice:

- The peak sidelobe level is $\boxed{20\log_{10}(n)}$
- The processing gain is $\boxed{10\log_{10}(n)}$

The sidelobe performance degrades rapidly away from zero-Doppler.

No Barker codes of length greater than 13 have been discovered. However, it is possible to concatenate codes together for greater length.

Processing Domain

We note here that processing can be carried out in either the time or the frequency domain. It is computationally more efficient to convert into the frequency domain by means of FFT, apply the replica spectrum and use the inverse-FFT to return to the time domain, as opposed to convolving the two signals in time.

Polyphase Codes

Greater flexibility over biphase codes (e.g. Barker codes) is provided by polyphase codes although the processing in generating and compressing is more complicated. Several have been proposed and studies, and most approximate linear FM. Examples include Frank codes, Kretschmer & Lewis P-codes, Costas codes and Welti codes.

Adaptive Correction for Phase and Amplitude Errors

It is possible to adaptively correct for phase and amplitude errors reducing the effect on range sidelobes. This is usually done digitally, by sampling the received radar pulses, comparing the received waveform with the desired waveform, and adjusting the next transmitted waveform to compensate for any errors. The new waveform is often stored in RAM and 'created' with a DAC.

Pulse Coding

Pulse coding using a 'broken FM' chirp waveform enables us to get very close to the -65dB assumed

achievable sidelobe levels. Higher FM rate 'wings' reduce Fresnel ripples and cancel far-side lobes. The improved DDFC waveform extends further to parametrise the waveform, and creates a continuous FM rather than piecewise (stepped gradients). It has a well behaved performance unlike the original pulse coding of Broken FM which had a chaotic function.

Doppler-Tolerant Waveforms

A waveform which allows a single pulse compression filter to be matched for all target velocities is:

$$u(t) = A(t) \cdot \cos\left[\frac{2\pi f_0^2 T}{B} \ln\left(1 - \frac{Bt}{f_0 T}\right)\right]$$

where $A(t)$ is a rectangular pulse, f_0 is the carrier frequency, T is the pulse duration, and B pulse bandwidth.

Differentiating with respect to time shows that the instantaneous frequency is:

$$\frac{1}{2\pi}\frac{d}{dt}\left[\frac{2\pi f_0^2 T}{B} \ln\left(1 - \frac{Bt}{f_0 T}\right)\right] = \frac{2\pi f_0^2 T}{f_0 T - Bt}$$

which is *linear period modulation* and not linear frequency modulation. If we expand the $\log$ out into a series and only the first two terms are taken, this reduces to linear FM once again:

$$u(t) = A(t) \cdot \cos\left(2\pi f_0 t + \frac{\pi B t^2}{T} + \frac{2\pi B^2 t^3}{3 f_0 T^2}\right)$$

Stepped CW Waveforms

Consider a linear stepped frequency pulse in which

τ_T	transmit sub-pulse length
τ_c	compressed pulse length
N	number of sub-pulses
f_k	frequency of the k[th] pulse
$\Delta f_s = f_k - f_{k-1}$	sub-pulse frequency step for $k = 1, \cdots, N$
$\Delta f = N\Delta_s$	total frequency excursion

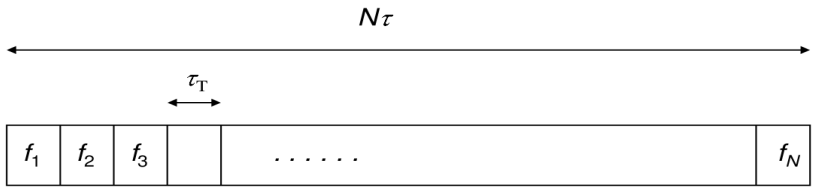

This is similar to the Costas code, but not random. The total bandwidth is

$$B = N \cdot \Delta f_s = \frac{N}{\tau_T}$$

So the range resolution is

$$\frac{c}{2B} = \frac{c\tau_T}{2N}$$

The pulse compression ratio is

$$\boxed{\frac{T}{\tau_c} = \frac{N\tau_T}{\tau_T/N} = N^2}$$

For a linearly stepped pulse, the Doppler characteristics are similar to that of linear FM.

FM Radar

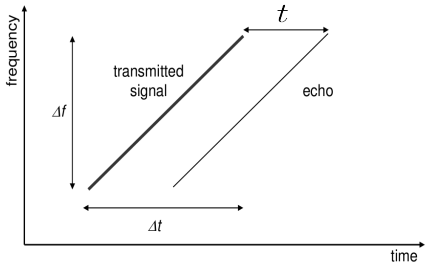

From the diagram to the right, the two-way propagation delay is

$$\boxed{t = \frac{2r}{c}}$$ (where t is time between echoes, and r range)

The Doppler frequency can then be calculated from the product of propagation time and the signal gradient, $\Delta f / \Delta t$.

$$\boxed{f_B = \frac{2r}{c} \cdot \frac{\Delta f}{\Delta t} = \frac{2\Delta f}{c\Delta t} \cdot r}$$

From this we can see that the range is a function of the frequency difference (beat frequency). The standard radar equation is

$$\boxed{\frac{P_r}{P_n} = \frac{P_t G^2 \lambda^2 \sigma L}{(4\pi)^3 r^4 k T_0 B F}}$$

The bandwidth of the spectrum analysis processing will be matched to the sweep duration. The appropriate value for B will therefore be the reciprocal of the sweep duration, $B = 1/T$, where T is the sweep duration, as opposed to the sweep bandwidth, Δf. This gives a processing gain equal to the time-bandwidth product of the waveform, just as with conventional pulse compression. With long, wideband frequency sweeps, the processing gain can be very large!

Moving Targets

We know that echoes from a target with radial velocity v towards radar will have a Doppler shift of

$$\boxed{f_D = \frac{2v f_0}{c}}$$

The frequency of the echo sweep will therefore be offset, leading to a delay error

$$\boxed{\Delta\tau = f_D \cdot \frac{\Delta t}{\Delta f}}$$ (relates time error, Δt, to a frequency error, Δf. See above diagram.)

This gives us a range error expression

$$\boxed{\Delta r = \frac{c\Delta\tau}{2} = \frac{\Delta t f_0 v}{\Delta f}}$$

Typically, a triangle wave frequency sweep is used. In doing this, the phase errors will invert sign between the up-sweep and the down-sweep, and so can be removed by averaging, thus reducing range error.

Issues Arising

A significant problem with CW radar is achieving sufficient transmit and receive isolation.

- Transmitter noise sidebands can swamp valid targets.
- Transmitter power leaking can desensitise the receiver.

The traditional solution is to use two separate antennas for TX and RX. Alternatively you can use a reflected power canceller (RPC).

Sweep Non-Linearities

Phase and amplitude noise in pulse compression pulsed radar systems was analysed by Klauder et al in 1960 using Fourier series and showing each term resulted in 'paired echo' range sidelobes. This allows for the maximum permissible phase or amplitude errors to be evaluated for a given range sidelobe level.

The situation with FM radar is different, and depends on the target range. Intuitively you can see that at zero range, sweep non-linearities will completely cancel.

Dynamic Range

As mentioned before, the inverse-fourth-power law means the echo signal strength varies greatly with range (doubling of range reduces signal by 12dB). We mentioned previously that we could vary the receiver gain thought the PRI to balance this inverse-fourth-power loss.

In FM radar the sensitivity time control (STC) can be applied in the frequency domain to the beat frequency signal; using a high-pass filter with a slope of 12dB per octave.

Synthetic Aperture Radar

The idea of synthesising a large antenna from a succession of spatial samples has origins in radio-astronomy. The idea of synthetic aperture radar was conceived by Carl Wiley in the USA in the 1950s in the context of sideways-looking radar. He realised that the variation in Doppler shift from echoes of a target meant that the beam-width of a sideways-looking radar could be artificially reduced by filtering. This is known as *Doppler beam sharpening* or *unfocused aperture synthesis*.

SAR Geometry

From the diagram on the right, we can find some of the parameters require by simple geometry

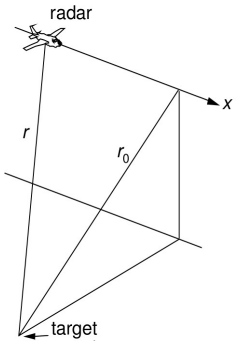

$$r = \sqrt[2]{r_0^2 + x^2}$$

$$r = r_0 \sqrt[2]{1 + \frac{x^2}{r_0^2}}$$

$$r = r_0 \left(1 + \frac{x^2}{2r_0^2} - \frac{x^4}{8r_0^4} + \cdots\right) \qquad \text{(series expansion)}$$

taking just the first 2 terms:

$$\boxed{r = r_0 + \frac{x^2}{2r_0}}$$

and

$$\boxed{\phi(x) = -\frac{2\pi}{\lambda} \cdot 2r}$$

So, in terms of phase we obtain

$$\boxed{= \phi_0 - \frac{2\pi x^2}{r_0 \lambda}}$$

or in terms of Doppler frequency

$$f_D = \frac{1}{2\pi}\frac{d\phi}{dt} \quad \rightarrow \quad \boxed{f_D = -\frac{2vx}{r_0\lambda}} \qquad \text{(Doppler is range of change of phase with time)}$$

Unfocused SAR Processing (Doppler Beam Sharpening)

Restrict the length of the synthetic aperture so that the maximum possible phase excursion is $\pi/2$ and add the echoes without any phase compensation. The length of the synthetic aperture comes from

$$\boxed{\frac{2\pi x^2}{r_0\lambda} = \frac{\pi}{2}}$$ This has the solution: $x^2 = \frac{r_0\lambda}{4}$ $\rightarrow$ $\boxed{x = \pm\frac{\sqrt{r_0\lambda}}{2}}$

So the length of the corresponding aperture is $\boxed{\sqrt{r_0\lambda}}$ and corresponding one-way foot-print is

$\boxed{r_0 \cdot \frac{\lambda}{\sqrt{r_0\lambda}} = \sqrt{r_0\lambda}}$. As this pattern is used on both transmit and receive, so the net resolution is

$$\sqrt{\frac{r_0\lambda}{2}}$$

Azimuth Resolution of Focused SAR

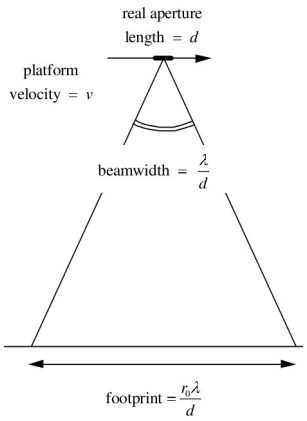

An Introduction to Radar Systems by *Merrill Skolnik* gives several methods for deriving the azimuth resolution of a focused SAR system. There is also a simple derivation, given here.

The Doppler resolution of the system is approximately $1/T$ where T is the time taken to form the synthetic aperture.

Doppler bandwidth corresponding to the target of azimuth extent Δx is

$$\frac{2v\Delta x}{r_0\lambda}$$

The minimum resolvable Δx over time T is therefore $\frac{r_0\lambda}{2vT}$, but as $T = \frac{r_0\lambda}{vd}$ we obtain

$$\Delta x = \frac{r_0\lambda}{2v} \cdot \frac{vd}{r_0\lambda} = \frac{d}{2}$$ (d is the real aperture length)

Range resolution is given as

$$\Delta r = \frac{2d^2}{\lambda}$$

Spotlight Mode

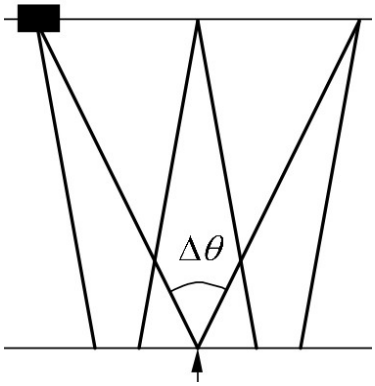

If the antenna can be squinted along-track (either mechanically or electronically), a given target scene of interest can be illuminated for a longer time creating a longer aperture, and hence giving higher azimuth resolution. This is referred to as *spotlight mode* in contrast to *strip-map mode*.

A more exact expression for azimuth resolution is

$$\Delta x = \frac{\lambda}{4\sin(\Delta\theta/2)}$$

For $\Delta\theta = \lambda/d$ this simplifies to $\Delta x = d/2$ as in the strip-map mode.

Assumptions

So far, we have made a few assumptions.

- We have assumed that the aircraft flies at uniform velocity in a straight line. If things like turbulence and roll are not taken into account the image will become unfocused.
- We have ignored higher order terms in the expansion of the phase history.
- We have ignored the fact that the platform have moved between transmission and reception of each pulse (the *stop-start* or *park-and-shoot* approximation).
- In the case of satellite SAR, the Earth's curvature will need to be taken into account.

Azimuth Ambiguities

If the real aperture is of length d, moving at velocity v we know that synthetic aperture is $\Delta_{az} = d/2$. We also see that the Doppler frequency is $f_D = \pm v/d$, depending on relation to bore-sight (– behind, + in front). Therefore, the Nyquist sampling theorem states that the PRF must be at least twice the largest Doppler frequency, so $\boxed{PRF > 2v/d}$ or $\boxed{PRF > v/\Delta_{az}}$.

Range Ambiguities

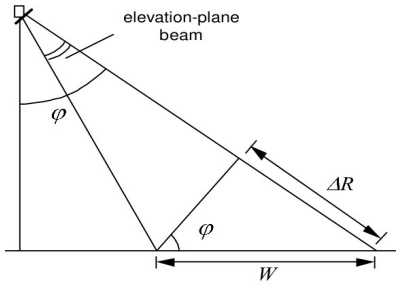

So for a sideways-looking system,

$\frac{c}{2R_{max}} > PRF$

and so

$$\boxed{\frac{c}{2W\sin(\varphi)} > PRF}$$

Azimuth Resolution in terms of Grating Lobes

We know that a phased array with an inter-element spacing of greater than $\lambda/2$ will exhibit grating lobe responses in addition to the principle one, at angles given by multiples of

$$\boxed{\sin(\theta) = \pm\frac{\lambda}{2s}} \qquad \text{(sample interval, } s = v \cdot PRF\text{)}$$

The first nulls of the real aperture pattern lie at directions

$$\boxed{\sin(\theta) = \pm\frac{\lambda}{d}}$$

So if we choose a real aperture length such that the grating lobes of the synthetic array lie beyond the first nulls of the real aperture pattern, then

$$\boxed{\frac{\lambda}{2v \cdot PRF} < \frac{\lambda}{d}} \quad \rightarrow \quad \boxed{PRF > \frac{2v}{d}}$$

Finite Suppression of Azimuth Ambiguities

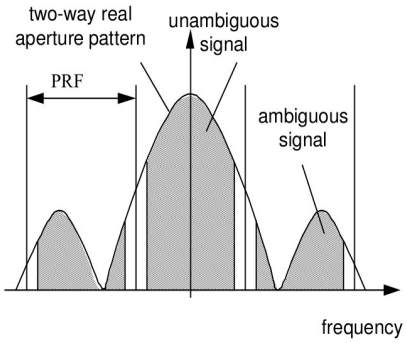

Due to the finite sidelobe levels of the real aperture azimuth, the azimuth ambiguities are not perfectly suppressed (nor in the elevation plane).

In azimuth (i.e. Doppler), aliased versions of the echoes appear, centred on multiples of the PRF. If the sidelobe level of the (two way) pattern of the real aperture is not sufficiently low, then aliased versions of strong targets may appear in the image.

Ambiguities and Antenna Area

The constraint can also be expressed in terms of the minimum antenna area:

$\frac{2v}{d} < PRF < \frac{2}{2W\sin(\varphi)}$

$W\cos(\varphi) = \frac{r\lambda}{a}$

hence,

$a \cdot d = \frac{4vr\lambda \tan(\varphi)}{c}$ [for the ERS-1 SAR, a factor of 2 was used]

The SAR Radar Equation

We need to distinguish between point targets and distributed targets, and between pulse level and image level.

Point Target

The single pulse received power is given by

$$\boxed{P_r = \frac{P_t G^2 \lambda^2 \sigma}{(4\pi)^3 r^4}}$$

At image level, if n pulses are used to form the synthetic aperture the echoes will add coherently (on a voltage basis) giving a gain factor of n^2, whilst the noise adds incoherently (on a power basis) giving a gain factor of n (ignoring losses and weightings). The net signal-to-noise power ratio in the image is therefore improved by a factor of n (n^2/n) over a single pulse.

Distributed Target

For a single pulse, the area of the resolution cell is given by

$$\boxed{r\Theta_B \cdot \frac{ct}{2\sin(\alpha)}}$$ (where t is uncompressed pulse length, and α is angle of incidence from vertical)

The received power is therefore

$$\boxed{P_r = \frac{P_t G^2 \lambda^2 \sigma^0 ct \Theta_B}{(4\pi)^3 r^3 2\sin(\alpha)}}$$

In the range compression process, the individual pulses are coherently added, so there is a corresponding gain. However, this is exactly balanced by the the reduction in the resolution cell area due to the pulse compression process. So there is no overall compression gain for a distributed target.

Noise Equivalent σ⁰

The sensitivity of a SAR is often quantified in terms of the noise equivalent σ^0 (NE σ^0), which is the value of backscatter coefficient (at maximum range) which would give a signal level equal to the receiver noise level.

Speckle

The radar equation predicts the mean signal level, but for a distributed target in a given pixel is a vector sum of all contributes from a large number of scatterers. According to the central limit theorem, the intensity will therefore be modulated by exponentially distributed multiplicative noise.

$p(I) = \frac{I}{I_0} e^{\frac{I}{I_0}}$

Or, if the signal is processed in the complex baseband form, Gaussian-based noise on both I and Q components. This gives a *speckled* grainy appearance to SAR images. This is normally combated by splitting the synthetic aperture into sub-apertures, forming separate images for each. These independent images (or *looks*) are joined to give a *multi-look* image of reduced speckle but reduced spatial resolution.

Optical SAR Processing

Since the synthetic aperture processing is effectively near-field focusing, it should not be surprising that you can do it optically. Before fast computers, it was: the echoes were down-converted and used to modulate intensity on a CRT screen. Each echo is recorded as a line on a strip of film, with successive echoes next to each other. Quadratic phase variation is matched (roughly) by an Fresnel zone plate. Other lenses may be used to correct for *walk* or *curvature*. Optical processing is cheap and has a high throughput rate, though there are shortcomings: radiometric calibration, low dynamic range and complex digitisation methods. There has been recent work on real-time electro-optic processing.

Digital SAR Processing

Echoes are lined up in memory. A slice is taken through the (complex) echoes at constant range, multiplied by phase weights (to taper side-lobes) and summed. Repeat for all azimuths, then all ranges. As mentioned before, it is typically done in the frequency (or Fourier) domain, due to better computational efficiency. For a medium resolution SAR system where range and azimuth compression are independent, we may define the following SAR processor:

Range Compression

FFT data samples in range

Multiply by range compression spectrum replica

Inverse FFT

Transpose data to by azimuth contiguous.

Azimuth Compression

FFT data in azimuth

Multiply by azimuth compression spectrum replica

Inverse FFT

Store or Display Image.

It's also interesting to note that a constant range has a curved nature, due to spreading of the beam.

SAR Imaging of Moving Targets

A moving target with a radial component of velocity, v_r results in an echo Doppler shift

$$\boxed{f_D = \frac{2v_r f_0}{c}}$$

The Doppler shifted sequence of echoes is matched-filtered (with a small mismatch) with an azimuth shift

$$\boxed{\Delta x = f_D \cdot \frac{r\lambda/d}{2v/d} = \frac{v_r r}{v}}$$

Terms: $Doppler\ shift \cdot \left(\frac{synthetic\ aperture\ length}{echo\ Doppler\ bandwidth}\right)$

This has the effect that moving objects are displaced from the background; an image of a train displaced from the track is shown. Also an image of a ship displaced from it's wash.

Autofocus

With airborne SAR, motion errors cause image distortion. The effects of these errors are:

- Along track

- Positional error displaced image
- Velocity error along-track scale change
- Acceleration variable along-track scale change

- Across track
  - Positional error displaced image
  - Velocity error image rotation
  - Acceleration variable image rotation

Autofocus constructs the correct matched-filter to remove these distortions, using the data itself. There exist several algorithms, including map drift, contrast optimisation, multi-look registration and phase gradient. When correctly used, the performance of these algorithms are comparable.

Contrast Optimisation

Each image is divided into strips. For each strip, the high-contrast range lines are selected. From these, we find the the *focus parameter* for the maximum contrast; hence we find the across-track acceleration. This is then integrated for platform displacement.

Phase Gradient Algorithm (PGA)

The method as published assumes the data was gathered over a single, long synthetic aperture as for spotlight mode.

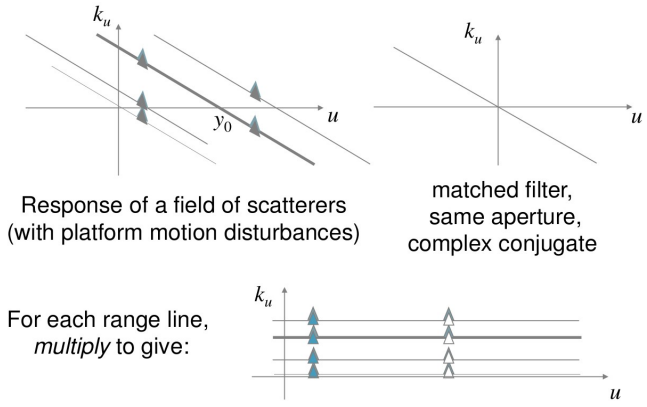

From this, we then take the along-track Fourier transform, select the strongest scatterer and move it to the origin. We apply windowing techniques to exclude all other scatterers. The inverse Fourier transform yields a signal $g(u)$ which depends on phase error $\phi_e(u)$: $g(u) = Ae^{j\phi_e(u)}$. The phase gradient can be readily calculated from $g(u)$ and dg/du. Integrate numerically to find $\phi_e(u)$ and hence extract the platform motion.

Moving Target Indication

Displacement Phase Centre Array, DCPA, uses two (or more) antennas arranged in tandem. By transmitting alternatively, and controlling the PRF as a function of platform velocity, it is possible to obtain two echoes from identical positions, displaced in time. If one such echo is subtracted from the other, static clutter should cancel, leaving only moving targets. In practise, this depends on antenna matching and motion errors. You may also use Space-Time Adaptive Processing (STAP).

Coherent Change Detection (CCD)

To detect whether or not a change has occurred, two images of the same scene are taken at different

times. They are geometrically aligned (so pixel-to-pixel they match), and then the images are checked for correlation. If nothing has changed, the pixels will be correlated. Where there is change, the pixels will have uncorrelated. Although this method can detect change, it cannot tell direction or magnitude.

Interferometric SAR

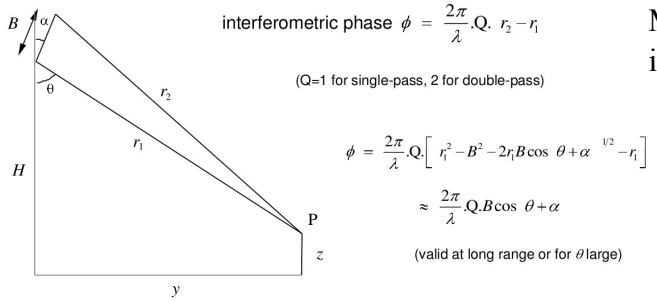

interferometric phase $\phi = \frac{2\pi}{\lambda}.Q.\ r_2 - r_1$

(Q=1 for single-pass, 2 for double-pass)

$$\phi = \frac{2\pi}{\lambda}.Q.\left[r_1^2 - B^2 - 2r_1 B\cos\ \theta + \alpha \ ^{1/2} - r_1 \right]$$

$$\approx \frac{2\pi}{\lambda}.Q.B\cos\ \theta + \alpha$$

(valid at long range or for θ large)

Measured parameters are r, H and ϕ, although ϕ is modulo 2π.

$$\boxed{r_2 = r_1 \cdot \frac{\phi\lambda}{2\pi}}$$

$$\boxed{\theta = \cos^{-1}\left(\frac{r_2^2 - r_1^2 - B^2}{2Br_1}\right) - \alpha}$$

Once θ is known, the target height can be found from $\boxed{z = Hr_1\cos(\theta)}$

We then get an *interferogram* from the target scene.

X-SAR

X-SAR/SRTM is one of the most important missions to planet Earth. The American Space Shuttle Endeavour, equipped with radar systems spent eleven days orbiting the Earth and collected data providing an almost complete map of the Earth's surface.

The main objective is the generation of a digital elevation model in 159 orbits; a requirement bought to the DLR's (German aerospace centre) attention following a national survey in 1995.

Differential Interferometry

Suppose we form two interferograms, separated in time, and the subtract one from the other. If the target scene has remained constant, the result will be a constant phase difference. If there has been any movement during the time, this will give interference fringes dues to changes in elevation. This is an extremely sensitive way of detecting elevation changes. An example here of the ERS-1 satellite to detect movements of 28mm from a satellite 1.2km away – surely a remarkable result!

Maximum Achievable Resolution – Spotlight Mode

Take the expression for the spotlight mode azimuth resolution

$\Delta x = \frac{\lambda}{4\sin(\Delta\theta/2)}$

A practical maximum value for $\Delta\theta$ may be $30°$, i.e. $\Delta\theta = 60°$. In this case, $\Delta x = \lambda/2$

In range, $\Delta r = \frac{c}{2B} = \frac{f_0\lambda}{2B}$

For a fractional bandwidth of 100%, $B/f_0 = 1$, so

$$\boxed{\Delta r = \frac{\lambda}{2}}$$ (with the possibility of resolution in the order of centimetres)

Polarimetric SAR

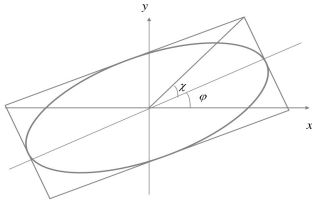

The way a target scatters for different polarisations gives important information. It can form an important part of the target signature for both

natural and man-made targets. There are various ways of describing the polarisation of an EM wave and of characterising the polarimetric scattering properties. Polarisation state can be specified by an orientation angle φ and ellipticity angle, χ.

It is also possible to use Stokes parameters written in vector form. Only three of the Stokes parameters are required, since they are related by
$I^2 = Q^2 + U^2 + V^2$

$$\mathbf{F} = \begin{bmatrix} \mathrm{I}_0 \\ \mathrm{Q} \\ \mathrm{U} \\ \mathrm{V} \end{bmatrix} = \begin{bmatrix} |\mathrm{E_v}|^2 + |\mathrm{E_h}|^2 \\ |\mathrm{E_v}|^2 - |\mathrm{E_h}|^2 \\ 2\,\mathrm{Re}\ \mathrm{E_v E_h^*} \\ 2\,\mathrm{Im}\ \mathrm{E_v E_h^*} \end{bmatrix} = \begin{bmatrix} \mathrm{I}_0 \\ \mathrm{I}_0 \cos 2\varphi \cos 2\chi \\ \mathrm{I}_0 \sin 2\varphi \cos 2\chi \\ \mathrm{I}_0 \sin 2\chi \end{bmatrix}$$

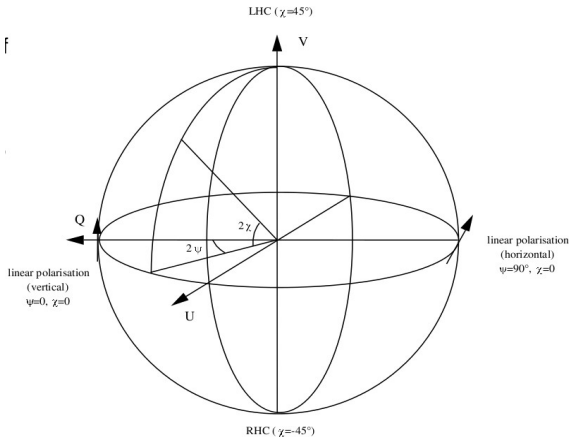

These components point to a point on a sphere of radius I_0. Coupling between states is $\cos(\zeta/2)$. Orthogonal states are diametrically opposed.

Polarimetric Scattering

The scattering matrix expresses how a target scatters energy as a function of polarisation.

$$\begin{bmatrix} E_v^s \\ E_h^s \end{bmatrix} = \begin{bmatrix} S_{vv} & S_{vh} \\ S_{hv} & S_{hh} \end{bmatrix} = \begin{bmatrix} E_v^i \\ E_h^i \end{bmatrix}$$

Where superscripts i and s refer to incident and scattered waves, respectively, and v and h vertical and horizontal components respectively. Another method is to use the polarisation response diagrams, which show co-polar and cross-polar signal levels for all incident polarisation states.

Polarimetric Radar

Requires an antenna system with both vertical and horizontal polarisation with good isolation between them, maintained over the full operating bandwidth and two separate receiver channels. Not an easy thing to make!

Transmit sequential horizontal and vertical pulses receiving both for each echo, thereby measuring each element of the scattering matrix separately. This gives 4 channels: HH, HV, VH, VV – for monostatic radar, HV and VH are identical. It is possible to use HH, HV and VV as separate *looks* to be combined to reduce speckle without degrading spatial resolution. Pre-whitening is often used before this, to make them statistically independent.

Inverse SAR (ISAR)

Instead of moving the radar platform, the radar may be kept stationary and the target moved. Two cases occur:

- Cooperative ISAR, in which the target motion (usually rotation) is controlled and known, used for high resolution RCS imaging.
- Non-cooperative ISAR, in which the target motion is not a *priori* known, and needs to be estimated.

In simple cases, such as rotation about a single axis, this can be done implicitly by (for example) using a ship roll to provide differential Doppler from target points at different heights.

In the general case, when *both* the target and the radar are moving the image can be obtained by Fourier transformation of spatial frequency (k-space) samples. But estimation of the unknown target motion parameters is still a problem – it can be tackled by autofocus-type techniques.

SAR Imaging of Ocean Waves

Ocean waves consist of long-wavelength swell waves ($\lambda \approx 100m$ or more) modulated by short wavelength ($\lambda mbda \approx 10cm$ or less) gravity/capillary waves. It takes about 1 second to synthesise a space-borne SAR, with the swell wave having a typical period of 8 to 20 seconds. Various mechanisms have been proposed to account for the imaging process:

- *Hydrodynamic modulation*: higher amplitude ripples at wave crest
- *Tilt modulation*: backscatter is highest from slope facing towards radar
- *Velocity bunching*: rising and falling portions of waves cause positive and negative Doppler shift and hence shift of energy in image.

The importance of these depends on the swell direction. A 2-D Fourier transform of the image of ocean waves gives the *Directional Wave Spectrum*, which shows the wavelength and direction of the swell components.

The Kelvin Wake

If wave propagation were non-dispersive with wave speed c and ship velocity V, then waves would appear stationary if they propagate at an angle

$\theta = \cos^{-1}\left(\frac{c}{V}\right)$

But waves propagate in deep water with a phase velocity:

$c = \frac{\omega}{k} = \sqrt{\frac{g\lambda}{2\pi}} = \sqrt{\frac{g}{k}}$

This tells us that we get different wavelengths, and hence different wavespeeds, c, for different angles θ.

However, waves propagate at the group velocity U and not at the phase velocity c. $U = d\omega/dk$.

$U = \frac{d\omega}{dk} = \frac{1}{2}\sqrt{\frac{g}{k}} = \frac{c}{2}$

This is interesting as it allows us to image the bottom topography of the seabed. Waves inside (internal wake waves) the water body are modulated and these modulate the surface wave, which our radar observes. Thus, with clever application, we can back compute the seabed topography.

Tracking Radar

Most of the radars we have looked at so far have been for surveillance – scanning an area and detecting the presence of targets. A tracking radar measures the coordinates of a target and provides data which may be used to determine the target trajectory and future location. It can be carried out in range, angle or Doppler. Angle is perhaps the most characteristic feature associated with tracking radar systems.

We can consider two types of tracking:

- **Track while scan**: Here the radar is in surveillance mode and attempts to form tracks of detected targets (although optimised for surveillance).
- **Continuous tracker**: Here the radar is dedicated to tracking. A surveillance radar may provide initial coordinates the tracker to avoid searching large areas. Often only a single target is tracked.

The objective of single target tracking is to continuously accurately measure a targets position, velocity and acceleration. There are four functions performed by tracking radar:

1. **Measurement**: determine the parameter set.
2. **Filtering**: processing of measurements to minimise error (multipath, noise, etc).
3. **Control**: generate command signal based on filtered information.
4. **Response**: reposition the antenna to the new target location.

As mentioned, tracking is done in range, Doppler and angle:

- **Range**: keep the range-gate centred on the target of interest. A series of range measurements are taken and used to predict the future range of the target, and to adjust the radar accordingly.
- **Doppler**: A Doppler filter is formed, e.g. by Fourier transforming a series of echoes to obtain target velocity and acceleration. This is used to improve new position estimates and to adjust the radar according.
- **Angle**: This is measured using lobing or mono-pulse techniques. The information is used to centre the antenna on (and to follow) targets, maintaining maximum power on it. A tracking loop measures differences between target echo location and antenna bore-sight and adjusts to reduce the difference.

Track While Scan

This can combine the tracking of multiple targets. As the radar scans, identified targets are registered and their parameters (range, range-rate, azimuth, elevation) estimated. For any one detection the estimates (many pulses per dwell) are collectively referred to as an *observation*. After many observations, the radar builds up accurate tracks of valid targets. There are 3 main components:

1. **Preprocessing**: Targets having the same range, range-rate and angle after successive scans are combined. They are transferred to a reference coordinate system.
2. **Correlation**: A prediction is made of the next target position based on previous observations. An example is the Kalman filter. Predictions are compared with measurements. If the prediction ties in with reality, then some more track is added. May require specific statistical tailoring
3. **Track Update**: Creation or Deletion. If a new observation is decided to not be part of this track, a new track is initiated. A second observation is used to confirm the track or delete it

if there is poor/no correlation. If there are no new observations after a while, the track is deleted.

Angle Tracking: Sequential Lobing

In sequential lobing the radar beam is switched between different positions in order to gain improved angular information about position. Consider two beams switched between the left and right of the target. If the target is directly between the two beams, then the signal strength in each beam will be equal. If the target it stronger in one beam than the other, the beams are moved such that they are equal, returning the target to the antenna bore-sight. This can be done using four horn antennas at a dish's focus point. Four pulses are fired, allowing observation in azimuth and elevation.

Angle Tracking: Conical Scanning

An alternative to sequential lobing is to rotate the antenna beam continually around the target. This is known as conical scanning. The angle error is detected and used to generate a correction voltage proportional to the tracking error with phase to phase to indicate direction. A servo takes the error voltage and moves the antenna in the direction of the target. The error signal may become very complex, especially if it is trying to predict future target motion.

Angular Tracking: Monopulse

Sequential lobing, conical scanning and their derivatives require more than one pulse to derive their error signals. There is an assumption that nothing changes between these pulses – in practise, target movement may make this assumption invalid. As the name implies, monopulse radar is able to derive error signals from a single pulse thereby avoiding such errors. There are two types of monopulse radar: *Amplitude Comparison* and *Phase Comparison*. Amplitude comparison is more common.

In 2D, monopulse uses two feeds to a parabolic dish, generating two overlapping beams. These are fed into a hybrid coupler (magic T) which provides a sum (Σ) and difference (Δ) patterns. The radar transmits via the sum input, and processes echoes via both ports.

Amplitude Comparison

This is the simplest form of monopulse radar. Two antenna beams are set at an angle to each other and their outputs connected to a hybrid coupler. The sum port has a higher signal-to-noise ratio and is therefore used for detection. The difference port produces an error voltage proportional to the targets offset from bore-sight. A phase sensor detects the direction to move though the amplitude determines how far. This method can be improved by taking the ratio of sum and difference channels to give a quotient independent of signal strength and linear against the error angle over a wider range. The overall improvement over a single beam is approximately ten-fold.

Phase Comparison

Here, instead of comparing amplitude of the echoes, we compare the phase of the echoes from two separate beams (or antennas). An echo on bore-sight will arrive at the two antennas at the same time and so will have no phase difference. An echo from a target at an angle θ from bore-sight will arrive at one antenna before the other, and therefore will create a phase difference due to the extra distance travelled.

The extra distance that one echo travels with respect to the other is given (from geometry) by

$X = d\sin(\theta)$ (where X is extra distance, d is antenna spacing, and θ is target angle)

This can be expressed as a phase difference, as

$\Delta\Psi = \frac{2\pi d \sin(\theta)}{\lambda}$ for small angles, $\sin(\theta) \approx \theta$

Range Tracking

In range tracking applications the target is tracked in range. Tracking can be done in range using early-late gate techniques. A higher echo will be observed in one of the gates unless the target is in the middle of them. The difference signal between the gates is a measure of the position of the target and the centre of the gates.

Doppler Tracking

Tracking radars are designed to extract Doppler information, such as CW or pulsed Doppler radar systems, can also track the Doppler frequency shift. This can be accomplished using a narrow band filter. This has two advantages:

(1) The signal-to-noise ratio is improved, especially if the Doppler shift is large in comparison to the clutter.

(2) It can resolve a target from a group which otherwise have the same angle as range.

Track Initiation

Consider a mechanically scanned radar. A target is detected. The next scan also confirms this target. A counter is incremented. If the target is not detected the next scan, the counter is decremented. If a predetermined number of counts is reached then a new target is declared. The target initiation schemes tend to be system specific and bespoke. We must also decide if two close tracks are the same target or separate.

Tracking Filters

The Alpha-Beta Tracker

The $\alpha - \beta$ tracker is a second order discrete time filter. It is the simplest of all the tracking filteres but contains the same basic ingredients as the more sophisticated versions. The equation for the first order (DT) filter is

$$\boxed{x_n = x_{n-1} + \alpha\Delta x}$$

where x_n is the new estimate of x

x_{n-1} is the previous estimate of x

α is the parameter that controls the length of memory ($0 \leq \alpha \leq 1$).

Δx is the error quantity (the difference between the estimate of x and measured x)

But the first-order filters follows a linearly changing quantity with a lag. We can maintain a similar estimate of the rate-of-change-of x and use it to correct the first order filter:

$$\boxed{\dot{x}_n = \dot{x}_{n-1} + \beta\frac{\Delta x}{\Delta t}}$$

where $\dot{x}_n$ is the new estimate of the rate-of-change-of x

$\dot{x}_{n-1}$ is the previous estimate of the rate-of-change-of x

β is the parameter of the same form as α ($0 \leq \beta \leq 1$)

Δt is the update interval of the filter

When we add this to the first order filter, we get

$$\boxed{x_n = x_{n-1} + \alpha\Delta x + \dot{x}_n\Delta t} \quad \text{where} \quad \boxed{\dot{x}_n = \dot{x}_{n-1} + \beta\frac{\Delta x}{\Delta t}} \quad \text{as before.}$$

This is the classical equation of the $\alpha - \beta$ tracker. The choice of parameters represent a compromise between the suppression of noise and the ability to track a manoeuvring target. You can see there is scope for a filter where α and β are updated automatically.

An $\alpha - \beta - \gamma$ filter attempts to deal with an accelerating target. Better still, use of a Kalman filter which in effect selects parameters of the filter which best match the dynamic behaviour of the target.

Tracking Errors

As is usually the case, the minimisation of tracking errors is usually a function of cost. Thus it is important to understand how much error we can tolerate. Error is split into two types:

- **External sources**: Such as those due to target fluctuations, clutter, multipath and atmospheric.
- **Internal sources**: Such as receiver noise, beam squinting and mechanical tolerances.

Target Fluctuation

These change the echo signal received and are caused by complex shaped targets. These are caused by the coherent nature of radar. The echo is the vector sum of all scatterers that make the complex target. A small change in relative viewing angle can cause big changes in the echoes. This can be very important in non mono-pulse, as two samples are used to calculate error.

Glint

We know that targets are make from a number of scatterers (see Swerling models). The way these scatterers add (as vectors) also gives rise to variation in the apparent direction of the echo – this may confuse the tracking radar.

A target consisting of two independent isotropic scatterers separated by an angle θ_D. Let the relative amplitude of the scatterers be a ($a < 1$), and the relative phase difference be α. The angular error in θ_D as measured from the larger of the two scatterers is

$$\boxed{\frac{\Delta\theta}{\theta_D} = \frac{a^2 + a\cos(\alpha)}{1 + a^2 + 2a\cos(\alpha)}}$$

Consider the case where $a = 1$ and $\alpha = \pi$ then $\Delta\theta/\theta_D$ tends to ∞. We see that the net echo shows that the echo is from outside of the physical dimensions of target! A real target may consist of more than two scatterers but the same principles apply. This can also be expanded to *range glint* and *Doppler glint*. Doppler glint may also be caused by motion of propellers, jet engines, etc.

Multipath

Multipath occurs when the radar pulses bounce of a surface (a building or the ground). If the ground (for example) reflects perfectly then the phase relationship between the two paths can result in constructive or destructive interference, depending on the heights of the radar and target. These cause nulls and maxima. Maxima can be up to 16 times more powerful than the direct signal, and the minima can cancel to zero. An effect can make it look like the target is underground.

Tropospheric Propagation

The troposphere is a inhomogeneous medium for propagation and will cause disturbance to the phase front of EM radiation. The most common is in heavy cumulus clouds which from columns of shaded air that are cooler than the surrounding air, resulting in changes of refractive index. The result is random beam bending.

Internal Sources

Thermal receiver noise of a tracking radar causes erroneous outputs of the angle error detector which can become significant at low values of signal-to-noise ratio. The rms angle error σ_t resulting is given by

$$\sigma_t = \frac{1.4B}{k_s\sqrt{BT(S/N)(f_r/\beta_n)}}$$

where k_s angle systems error detection slope

θ_B antenna 3dB beamwidth

S/N signal-to-noise power ratio

f_r pulse repetition frequency (PRF)

β_n servo bandwidth

B receiver bandwidth

T pulse width

There are other sources of internal noise too, such as pedestal bending, gearing backlash, bearing wobble and other mechanical imperfections.

Multifunction Radar

These offer potential for wide area search and tracking functions combined into a single system due to the non-linear strategies afforded by electronic scanning. The advantages of using a phased array (electronically scanned beams) for tracking is that targets can be acquired quickly and put into track even when the system is already tracking many targets. This makes phased arrays affordable as they replace many radars with one system.

Elimination of mechanical scanning allows for rapid movement of the antenna beam from one target to another. Track updates can be tailored to individual targets and their conditions. The illumination pattern of the antenna may also be adjusted. However, phased arrays exhibit high angular accuracy that deteriorates away from bore-sight.

Multistatic Radar

The integration of tracks from several radar systems located at different sites offers a number of potential performance benefits. It offers a common picture of radar activity, vital for applications such as air traffic control. It is more effective under hostile jamming conditions. Several track integration methods:

1. **Track selection**: generate a track with each radar and choose the best
2. **Average track**: generate a track with each radar and then average
3. **Augmented track**: choose one radars track, and update with all radar information
4. **Detection to track**: use all radar detections to update the system track

Theoretically, the detection to track method yields the best results. However, corrupt data can

reduce performance and care has to be taken to weigh the inputs appropriately. This can be extended to sensors other than radar.

Aviation Radar and GNSS

Primary ATC Radar

Primary ATC radar can be used for a variety of tasks from approach control to long range surveillance. The following bands are used for avionics radar:

Long range & airfield surveillance	1 – 3 GHz
Surface movement radar (SMR)	9 – 16 GHz
Terminal weather radar	1 GHz or 3 GHz (not used much in UK)

The main characteristics of these types of radar will be described briefly in subsequent sections.

Long Range Surveillance

Surveillance radar may be used for both tracking of aircraft in airways (in main flight) and in surveillance of terminal areas (airport approach). Current systems mainly use L-band (1 – 2 GHz) and S-band (2 – 4 GHz). Many ATC radars combine primary and secondary radar (detailed later).

Surface Movement Radar (SMR)

Higher air traffic densities are leading to an increased density of aircraft on approach and take-off. This in turn results in severe demands on ground movement control to allow the high density of ground movements required in consequence. One of the requirements of the new European air traffic management system for year 2000+ is for improved surface management systems and resources. Surface surveillance will thus become even more safety critical as traffic density grows. Over 200 runway incursion accidents occur in the USA every year and several serious world-wide in the last few years have been due to lack of proper surface movement surveillance and control.

[SMR not examined in 2011 season]

Terminal Weather Radar

Suitably designed weather radar can give information on many meteorological phenomena of interest to air traffic control centres. These include identification of areas of heavy rain or storms, icing and severe turbulence. Such information, delivered in close to real time can assist controllers in applying re-routing strategies to avoid congestion and increase safety margins. Little work on weather radar for aviation specific application has been carried out in Europe; with most work done in the USA.

Weather radar measures backscatter from collections of *hydro-meteors* (rain, snow, hail, etc) in the atmosphere. To calculate the RCS of a collection of hydro-meteors we use the following equation:

$$\sigma_{scatt} = \frac{C\pi^5}{\lambda^4} \sum_{i=1}^{N} D_i^6$$

where σ_{scatt} is the RCS of the collection of hydro-meteors, in m^2

C is a dimensionless constant depending on dielectric constant of hydro-meteors

D mean diameter of particles

λ radar wave-length

N number of scatterers per volume illuminated

$C \approx 1$ for water. In practice, a reflectivity factor (Z) is usually used to quantify the returned signal,

where

$$\boxed{Z = \frac{\sum_{i=1}^{N} D_i^6}{unit\ volume}}$$ (where Z is in units $mm^3 \cdot m^{-3}$)

or

$$\boxed{Z = ar^b}$$

where r is precipitation rate and a and b are dependant on the hydro-meteor type, as in the following:

Precipitation	a	b
Rain	200	1.6
Ice Crystals	500	1.66
Wet Snowflakes	2000	2
Dry Snowflakes	1500	2

If the volume of the resolution cell is

$V_{res} = (R\Delta\theta)(R\Delta\phi)(c \cdot t/2)$

then the RCS of the cell is

$\sigma = V_{res} \sum \frac{\sigma_{particle}}{unit\ volume} = \frac{C\pi^5}{\lambda^4} Z R^2 \Delta\theta\Delta\phi\frac{ct}{2}$ $[m^{-2}]$

By using Z in the radar equation the power returned (P_r) from precipitation can be calculated. This is only valid up to about X-band as Z is not frequency dependant in this range. Combining constants together and assuming $C = 1$

$$\boxed{P_r = \frac{2.3 \times 10^{-11} P_t G_t G_r Z \Delta\theta\Delta\phi L_{sys} L_{atmos}}{\lambda^2 R^2}}$$ (L losses are system and atmospheric)

In addition to the returned power, the returned polarisation is also important. Design issues are dependant on specific requirements, but typically for aviation weather detection we need: sensitivity, range ambiguity and decorrelation, beam-shape and volume sampling.

Sensitivity

The minimum reflectivity of interest at a typical range of 150km is about 30dBZ. A probability of detection (P_d) of around 0.95 and a false alarm probability (P_{fa}) of 10^{-6} for a +30dBZ target in a single resolution cell are typical requirements.

Range Ambiguity & Decorrelation

There is a trade-off between the maximum unambiguous range, the maximum unambiguous Doppler shift, the number of independent samples per resolution cell and the time required to sample the volume of interest. The unambiguous range is probably more important to avoid aliasing of distant precipitation into the terminal area.

To cover the terminal area out to a range of typically 150km, and allowing time for TX/RX switching the maximum PRF is approximately 1KHz but this has two problems:

- Targets beyond 150km are aliased into the terminal area.
- Samples could not be independent; the decorrelation time of precipitation targets at C-band

is typically 10ms dropping towards 5ms in heavy rain.

A solution is to use a PRF with carrier frequency shifts to decorrelate the returns from successive pulses; the frequency shifts repeating every 5 – 10 pulses.

Beam-shape & Volume Sampling

To give sufficient height resolution at long range, a pencil beam must be used with high elevation scan rate. A typical 1° beam-width gives a 2.6km height resolution. Two methods of sampling in elevation can be used:

- Electronically scan the beam in elevation and mechanically in azimuth.
- Use a number of fixed beams in elevation with the beam-width increasing with elevation and sampling the beams simultaneously or sequentially.

Secondary Surveillance Radar (SSR)

SSR is not a true radar system but a two-way communications system between an interrogator on the ground an a reply transmitter fitted on the aircraft. However SSR is very similar in operation to conventional radar and suffers many of the same problems and limitations. SSR is now one of the most frequently used radar controller aids for ATC. Unlike primary radar it requires aircraft to carry a reply transmitter called a transponder. Most commercial aircraft are required to be fitted with this equipment for transit through controlled airspace.

Advantages

The system has a number of advantages:

- The ground transmitter needs only a relatively low power.
- The returns, not merely reflections, are of superior signal strength and reliability.
- The returns form the aircraft can be coded to pass information to the ground station.

Pulse Pattern

The interrogating transmitter radiates on a frequency of 1030 MHz, with a pulse pattern as shown right. The main lobe transmits pulses P1 and P3. The control transmission P2 is sent via a second antenna. The second antenna must have a gain greater than that of the side-lobes. The transponder is set to reply if P2 is less than 9dB lower than P1, thus suppressing sidelobe returns.

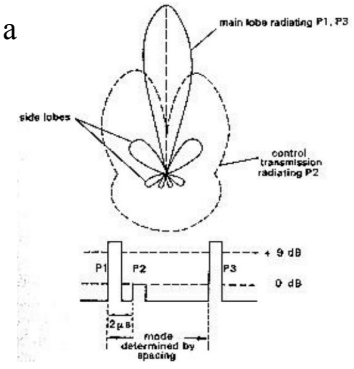

The timing interval between P1 and P2 is fixed at $2\mu S$. The P1 to P3 spacing is varied according to required mode, in accordance with the following table:

Mode	P1-P3 Spacing (μS)	Application
A *	8 ± 0.2	Civil ATC
B	17 ± 0.2	Military ATC
C *	21 ± 0.2	ATC + Altitude
D	25 ± 0.2	Unassigned

(starred items refer to modes most commonly used *)

Transponder

On receiving a valid interrogating pulse, the aircraft radiates two framing pulses $20.3\mu S$ apart. Between these are the information pulses. Up to 13 information pulses may be sent divided into 4 groups of 3 plus one unassigned pulse (X). Each pulse in each group is identified by a subscript number from 1 to 4 so that an octal system of coding is possible with codes from 0000 to 7777. Mode C reporting is done automatically when requested by a separate pressure capsule in the equipment. The binary code is called a Squark code. Certain internationally agreed codes are used for emergency or urgency situations:

7700 Distress or emergency

7600 Radio failure

7500 Unlawful interference or hijacking

Display

The aircraft is displayed on the controllers radar screen with an attached label (the Track Data Block). The TDB can show:

- Squark code (or airline flight code, aircraft callsign if a flight plan has been filed)
- Aircraft actual height information derived from the SSR downlink
- Cleared exit flight level and exit flight level from controllers sector
- Aircraft ground-speed downloaded from the aircraft systems.

The aircraft's track history is also shown allowing for a quick visual estimation of aircraft's speed and direction.

Range

Range *uplink* is given by

$$R^2(max) = \frac{P_i G_i G_t \lambda_i^2}{(4\pi)^2 S_t L_i L_t L_a}$$

Where P_i Peak interrogator power.

G_i, G_t Antenna gains for interrogator and transponder, respectively.

λ_i Interrogator wave-length.

S_t Minimum received power to produce reply (watts).

L_i, L_t, L_a Losses in the interrogator, transponder and atmosphere respectively.

This is the same for the *downlink* with the obvious parameters reversed (i.e. the transponder transmits, and the S_t is replaced with S_i, the power required to decipher the transponder response, in watts). We also note that the ERP can be substituted, $ERP = P_i G_i / L_i$. The ICAO sets the limit for ERP: -52.5dBW for the interrogator, -27dBW for the transponder. This corresponds to an uplink of around 200 nautical miles.

Antenna

Early SSR used the 'hog trough' antenna – 4 meters horizontal aperture, 0.5 meters vertical aperture. This results in a large vertical beam-width, causing large ground reflections. Newer designs use a Large Vertical Aperture (LVA) antenna with a 1.6 meter vertical aperture resulting in a much narrower vertical beam-width. These antennas are often co-mounted with (above) the primary radar

antenna.

Accuracy & Limitations

The main limitations with SSR:

1. Wide beam-width in vertical and horizontal planes results in heavy ground returns and *track wander*. These problems are largely overcome with the LVA antenna mentioned in the above section.
2. Interference due to aircraft replying to two different ground stations, called *fruit*.
3. Overlapping replies of two or more aircraft in close proximity within the same antenna beam-width, called synchronous *garble*.

Due to the projected increase in air traffic in the future it is expected that the current SSR system will saturate with fruit and garble eventually. Future developments are under way to develop an SSR system with increased accuracy and capacity, free from fruit and garble. The latest development is called *Mode S*.

Mode S

The main benefits of Mode S are:

- Unambiguous aircraft identification
- Improved integrity of surveillance data
- Elimination of synchronous garble
- Improved air picture and tracking in horizontal and vertical modes.
- Alleviation of Mode 3/A code shortage
- Increased target capacity

It allows aircraft to be identified more accurately in terms of height. This reduces problems with overlapping tracks when many aircraft are in holding patterns. There are two types of operation being deployed: Elementary Surveillance (ELS) and Enhanced Surveillance (EHS).

Elementary Surveillance (ELS)

Aircraft compliant with Mode S ELS provide the following: Automatic reporting of aircraft identity, transponder capability report, altitude reporting in 25ft intervals, flight status (airborne/on ground) and SI code capability (a technical function to identify transponders compliance with surveillance identifier (SI) code).

Enhanced Surveillance (EHS)

Aircraft compliant with Mode S EHS provide the following in addition to that of ELS: Selected altitude, roll angle, track angle rate, true track angle, ground speed, true airspeed, magnetic heading, indicated airspeed and vertical rate (climb/descend rate).

Global Navigation Satellite Systems (GNSS)

GNSS is the generic term for satellite navigation systems that provide autonomous geo-spatial global positioning. The original GPS was developed for military purposes by the USA in the 1970s. Currently only the US NAVSTAR GPS and Russian GLONASS systems are fully operational. The EU GALILEO and Chinese COMPASS GNSS systems are due for completion over the next 5 to 10 years.

NAVSTAR

Positioning requires a highly accurate clock timing and synchronisation – satellites have an on-board caesium clock maintained by a master control station. Two frequencies are used to radiate the navigation signal:

L1 1575.42 MHz

L2 1277.60 MHz

Two main modulations are used:

P	Precise	10.23 MHz	Highly accurate military service
CA	Course/Acquisition	1.023 MHz	Original civilian service (less accurate)

CDMA signal coding is used due to the high resistance to interference. Each satellite transmits a navigation message containing: Orbital data, clock behaviour, system time, satellite status. It offers the following services:

Standard Precision Service (C/A code) - SPS

100m horizontally

156m vertically

Precise Precision Service (P code) - PPS

22m horizontally

28m vertically

PPS is degraded to SPS by *Selective Availability* (SA). This is achieved by degrading the clock signal, typically introducing *dither* (phase noise). This dither was removed by DOD2000, upgrading the SPS service to PPS. It could be introduced again.

The system has 24 operation satellites in 6 orbital planes. Circular 20,200km orbits within a 12 hour period. Spacecraft – 3-axis stabilised with dual solar arrays. S-band telemetry channels. Specified design life, 5 years (they have lasted much much longer). There are 3 monitor stations, 3 ground uplink antennas and one master control station (2nd space operations squadron at Falcon AFB, Colorado, USA). The master controls station receives data from all other stations, and checks orbits/updates satellite's navigation message. System time is referenced to master clock at USNO (US Navy Observatory – The US equivalent to Greenwich, UK) with a maximum deviation of $1\mu S$.

The user segment (your device) is a small omni-direction unit. The receiver/processor is a complex high-speed processor. The GPS signal is usually significantly below the noise floor – this is a strong reason for using CDMA.

GLONASS

Navigation system operated by Russian Space Forces for Russian Government. Development begun in 1976 – fully up in 1995. System fell into disrepair until 2001, when the Russians repaired it, and it is now fully operational. Several updates of satellites taken place, with latest GLONASS K. On-board caesium clock accurate to $1\mu S$. L-band navigation systems in two bands; 1602.5625 – 1615.5 MHz and 1240-1260 MHz. ERIP 25 – 27dBW. Two modulations; C/A with 100m accuracy and P with 10 – 20m accuracy. 24 satellites in 3 orbital planes – scheduled to be increased to 30 by end of 2011 (unsure if this has yet happened). 19,310km orbit with 11hr 15m period. FDMA signalling (not CDMA as NAVSTAR). Code rates; C/A of 0.511Mbit/s and P of 5.11Mbit/s. CDMA has been added to support compatibility with NAVSTAR and existing GPS equipment (2006).

GALILEO

Galileo is Europe's own GNS system, providing high accuracy and under civil control. Planned to be inter-operable with GPS/GLONASS. Offering dual frequencies and real-time positioning accuracy down to the metre range – a high accuracy publicly available system. First experimental satellite GIOVE-A was launched 28/Dec/2005 – completed all tests successfully – now transmitting navigation signals. GIOVE-A2 was launched in 2008. Thereafter, four operational satellites – the basic minimum requirement for satellite navigation in principle – will be launched in 2011 to validate the Galileo space and ground segments. Once this is all verified, the rest of the satellites will be installed to get full operational capacity. 3-axis stabilised with 600kg dry mass. 700W from 2 sun-tracking solar panels. Butane propulsion system. Two redundant, compact rubidium atomic clocks with stability of $10nS$ per day. Once fully deployed, will have 30 satellites, 27 in use, 3 spare (active) positioned in 3 medium Earth orbit planes. Orbits at 23,222km.

BEIDOU-1

This is the first experimental Chinese positioning system based on 3 or 4 satellites. 4 satellites are thought to have been launched between 2000 and 2007. Thought to be operational to an accuracy of 10m for Chinese users.

COMPASS

Also known as BEIDOU-2 or BD2. This is a project by China to develop an independent global satellite system. This will be similar to NAVSTAR and GALILEO. Planned 5 GEO and 30 MEO satellites. Military and Civil services offered. Frequencies may overlap with Galileo and inter-system interference may be an issue.

GNSS Precision Approach and Landing

GNSS is increasingly being used as an aircraft landing aid at airports without approach radar. Many such systems use *differential* GPS which involves the use of a reference ground station to increase accuracy. Due to safety concerns a lot of research has been carried out into the accuracy and integrity of the GNSS signal both on-board the aircraft and at the ground station. Several systems are being developed to augment GNSS signals for aviation use with a network of ground stations. The main purpose of these systems is to improve accuracy of the GNSS positioning in 3D over large areas. This systems include: The Wide Area Augmentation System (WAAS), USA; The Multi-function Satellite Augmentation System (MSAS), Asia; The European Geostationary Navigation Overlay Service (EGNOS), Europe.

EGNOS

The EGNOS system consists of three geostationary satellites and a network of ground stations. It has shown better than 2m accuracy and should be in full service by 2011.

GPS

Accuracy

There are two main sources of error:

1. **Multipath**: Caused by reception of signals reflected from surrounding buildings, terrain, airframe components, etc. Causes gradual degradation of the signal accuracy.
2. **Interference**: Can come from internal or external sources, including deliberate jamming or spoofing and solar weather. This reduces the signal-to-noise ratio of the received signal at

the receiver, causing an abrupt failure of the system.

Multipath at the Airborne Receiver

Airframe reflections from other parts of the aircraft structure may cause signal delays – these are usually less than $20ns$ due to short distances. Values of error around 20 – 60 centimetres. For coherent phase detection, mean errors of around 1 centimetre are expected.

Ground or obstacle reflections become important as the aircraft approaches the ground during landing as the geometry changes quickly. These can be eliminated with a coherent detector.

Multipath at the Ground Station

Differential GPS relies on a ground station for reference. Multipath at the ground station is a significant source of error. Filtering is difficult due to the static environment. The main errors are due to reflections from buildings and obstacles as well as ground reflections.

Multipath Mitigation Techniques

There are several techniques used to mitigate multipath on GPS:

- Correlation process enhancement
  - Narrowing the correlator spacing
  - Estimating parameters of each multipath signal via maximum likelihood algorithm (This can reduce errors by 10 – 40%)
  - Estimating tracking error from slope of correlation factor. Uses feedback to ensure correlation is centred on peak. Can reduce errors by 25 – 50%.
  - None of the above will work for short delays; less than 0.1 chip or 30m
- Carrier Smoothing
  - Smoothing code measurements with carrier measurements using a filter
- Path Diversity
  - Use different paths to combine signals and thus improve signal to noise ratio
  - Space diversity uses a network of ground reference stations or multiple receive antennas
  - Frequency diversity uses a weighted average of L1 and L2 signals of the P-code

Interference

This is mainly a problem on the airborne receiver. The effect is to reduce the signal-to-noise ratio – this effects the integrity causing the GPS reception to abruptly fail, as opposed to multipath which causes the GPS to loose accuracy. Main problems caused by on-board sources such as the aircraft's VHF radio (harmonics in the GPS band), SatCom radio (intermodulation with in-band and out of band interference) and mobile satellite radio (MSS) which is in-band at 1610 – 1626 MHz (>100 KHz modulation) and 1574 – 1575 MHz (CW).

Interference Mitigation Techniques

As with GPS multipath, there are a few techniques to help reduce GPS interference:

- At the receiver
  - Detection by measurement of parameters such as control voltage or correlator power

    - Pre-correlation techniques
    - Post-correlation techniques
- Out of band filtering

Summary

- Multipath affects the accuracy of the signal, whereas interference seems to be more related to the integrity of the GPS lock.
- Multipath requires the use of a narrow spacing correlator, carrier smoothing, careful antenna design and diversity techniques.
- Interference can easily be filtered. Only MSS interference is a real problem as it is in-band.
- Another way of solving these issues would be to combine GPS with other signals using data fusion techniques.

Phased Array Radar

Introduction

What is the purpose of an antenna?

- It provides a good impedance match between the transmitter (or receiver) and free space.
- It provides angular directionality and gain for the transmission or reception of plane waves.

Phased array (or electronically scanned) antennas provide rapid, flexible beam pointing without inertia. They can carry out multiple functions and vary 'dwells' and 'update rates' on an individual target basis.

The Parabolic Dish Antenna

The parabola has the property that an incident plane wave will be reflected to a single (focal) point. Placing the receiving (or transmitting) element at this point leads to efficient energy collection.

Equation of a parabola: $\boxed{y^2 = 4fx}$

The differential path lengths determined by the parabolic shape ensure that the plane wave is bought to focus (i.e. everything arrives at the focal point in phase). This is a fundamental feature required in all antennas. It's just that a phased array antenna does this electronically!

Comparison with Phased Arrays

The differences between mechanically scanned dishes and phased array are detailed below. Items with + are desirable properties, while those with a – are not.

Mechanically Scanned	**Phased Array**
– Scan rates and beam patterns are limited by mechanical inertia	+ Electronically scanned: rapid and intertial-less. Limited by phase-shifter speed ($\approx ms - \mu s$)
+ Constant beam-width with look angle	– Beam-width changes with look angle
+ Constant gain with look angle	– Gain changes with look angle
– Fixed beam pattern	+ Variable beam pattern
+ Simple proven technology	– Complex (but proven) technology
+ Low cost	– Expensive, but falling cost
	+ Transmit power can be distributed

The Array Antenna

An array antenna consists of a number of smaller antenna elements connected together so that they replicate an single large antenna. Equal path lengths to each results in a beam normal to the array face. Changing the path length relationship between antenna elements enables the beam to be pointed in a different direction. Hence sequential changes of path length leads to beam scanning similar to that of mechanically scanned radar.

Note: The beam-width at bore-sight (in radians) at the 3dB point is given by $\lambda/L = \lambda/Nd$, where L is array length, N is the number of elements, and d the inter-element spacing (distance between each antenna element).

Phased Array Theory

In a two element array, cancellation occurs due to cancellation of wave-fronts being $180°$ out of phase. Therefore, a null occurs in the *far field*. Reinforcement will also occur where the two wave-fronts are perfectly in phase and the sources add coherently.

The time varying phase of the electric field propagating at a frequency f is given by $e^{j2\pi ft}$. The electric field undergoes a 2π rotation in phase every $1/f$ seconds (or every λ/c).

Consider a set of N identical elements whose phase centres are aligned along an axis, with uniform inter-element spacing, d. The elements are fed by a matched feed network according to an illumination function defined by a set of complex numbers:

$a_0, a_1, a_2, \ldots, a_n, \ldots, a_{N-1}$ (a_0 to a_{N-1} is N elements, a_n being one element in the middle)

Each element has the same pattern, $f(\sin(\theta))$.

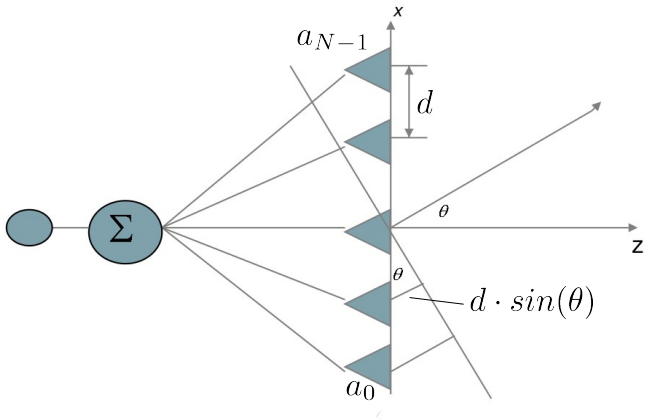

Using the principles of superposition, the far-field pattern of the array $F(\sin(\theta))$ on receive is obtained by summing the voltage contributions from each of the elements:

$$F(\sin(\theta)) = \sum_{n=0}^{N-1} a_n \cdot f(\sin(\theta)) \cdot e^{j\frac{2\pi}{\lambda} nd\sin(\theta)}$$

$$F(\sin(\theta)) = f(\sin(\theta)) \cdot \sum_{n=0}^{N-1} a_n \cdot e^{j\frac{2\pi}{\lambda} nd\sin(\theta)}$$

The fact that we can take the element pattern $f(\sin(\theta))$ outside the summation means that we can express the array pattern as the product of the element pattern and the array factor.

If the array illumination is uniform and with constant phase gradient φ from one element to the next, then we can write

$a_n = e^{-j\varphi}$

and the array factor becomes

$\sum_{n=0}^{N-1} \exp\left(jn\left(\frac{2\pi}{\lambda} d\sin(\theta) - \varphi\right)\right)$

we let $x = \exp\left(j\left(\frac{2\pi}{\lambda} d\sin(\theta) - \varphi\right)\right)$

and we recall that

$\sum_{n=0}^{N-1} x^n = \frac{x^N 1}{x1} = x^{N-1/2} \frac{x^{N/2} x^{-N/2}}{x^{1/2} - x^{-1/2}}$

So taking the constant amplitude factor, $Nx^{N-1/2}$ the array factor can be written as

$$\frac{\sin\left[N\left(\frac{\pi d\sin(\theta)}{\lambda} - \frac{\varphi}{2}\right)\right]}{N\sin\left(\frac{\pi d\sin(\theta)}{\lambda} - \frac{\varphi}{2}\right)}$$

often $$AF = \frac{\sin(Np)}{N \cdot \sin(p)}$$

where $$p = \frac{\pi d}{\lambda}\sin(\theta) - \sin(\theta_L)$$

(θ_L is the beam angle, $\sin(\theta)$ is the variable, d the inter-element spacing, and λ the wavelength)

Array Factor – Properties

- Periodic
- Defined for any value of $\sin(\theta)$, even for $|\sin(\theta)| > 1$ which we interpret as the imaginary or

invisible domain.

- Passes through a maximum of ± 1 every time the denominator and numerator are simultaneously equal to zero, i.e. when

  $\sin\left(\frac{\pi d \sin(\theta)}{\lambda} - \frac{\varphi}{2}\right) = k\pi$ (where k is integer)

- A maximum is obtained in direction θ_0 when

  $\sin\left(\frac{\pi d \sin(\theta_0)}{\lambda} - \frac{\varphi}{2}\right) = 0$

  i.e. such that

  $\varphi = 2\pi \frac{d}{\lambda} \sin(\theta_0)$

- As $N \to \infty$, the function tends to the well known 'sinc'
- First side-lobe is at approximately $-13dB$
- Power pattern is proportional to the square modulus of the voltage pattern

Grating Lobes

Since the array factor is periodic, there is the possibility of more than one principle maximum within the visible (real) domain. This is undesirable, both because of the directional ambiguity and on transmit, the power is wasted in unwanted directions. But a directional element pattern will attenuate grating lobes close to the imaginary domain. The worse case occurs when the beam is scanned to some maximum angle, θ_M. The condition for the grating lobe on the other side still to lie in the imaginary domain is

$$\boxed{\frac{d}{\lambda} < \frac{1}{1 + \sin(\theta_M)}}$$

As an example, for $\theta_M = 30°$, $\sin(\theta_M) = 1/2$, so $d/\lambda < 2/3$.

Beam-width

The -3dB beam-width can be found by setting

$$\frac{\sin\left[N\left(\frac{\pi d \sin(\theta)}{\lambda} - \frac{\varphi}{2}\right)\right]}{N \sin\left(\frac{\pi d \sin(\theta)}{\lambda} - \frac{\varphi}{2}\right)} = \frac{1}{\sqrt{2}}$$

which is obtained approximately when

$$N\pi \frac{d}{\lambda} \left[\sin\left(\theta_0 + \frac{\theta_{3dB}}{2}\right) - \sin(\theta_0)\right] = \frac{\pi}{2}$$

from which

$$\theta_{3dB} \approx \frac{1}{\frac{\pi d}{\lambda} \cos(\theta_0)} = \frac{\lambda}{Nd \cos(\theta_0)} = \frac{\lambda/L}{\cos(\theta_0)}$$

The instantaneous bandwidth is conventionally defined as the change in frequency for which the change in pointing direction is equal to the -3dB bandwidth:

$$\frac{df}{f} = \frac{1}{\sin(\theta_0)} \frac{\lambda}{L} \quad \text{or} \quad df = \frac{1}{\sin(\theta_0)} \frac{c}{L}$$

This does not depend on the centre frequency, but on the length, L, of the array. The band-width can be considered as the inverse of the time taken for the signal to traverse the aperture.

Phased Array Theory... Some more parameters

$$SL_{ave} = \frac{P_s}{\Omega_s} \times \frac{4\pi}{P_t}$$

$$SL_{ave} = \frac{P_t P_{mainbeam}}{4\pi - \Omega_{mainbeam}} \times \frac{4\pi}{P_t}$$

$$SL_{ave} = \frac{1 P_{mainbeam}/P_t}{1 - \Omega_{mainbeam}/4\pi}$$

$$SL_{ave} \equiv 1 P_{mainbeam}/P_t$$

Where

SL_{ave}	average side-lobe level with respect to isotropic.
P_s	power in the side-lobes
P_t	the total power
$P_{mainbeam}$	power in the main beam
Ω_s	steradian area of the side-lobes
$\Omega_{mainbeam}$	steradian area of the main beam

Aperture Tapering

The pattern at bore-sight is given by

$$\frac{\sin\left[N\left(\frac{\pi d \sin(\theta)}{\lambda}\right)\right]}{N \sin\left(\frac{\pi d \sin(\theta)}{\lambda}\right)}$$

The peaks of the first side-lobes occur at a value of approximately 13dB below the main peak. Therefore objects off bore-sight that are 13dB stronger than an object on bore-sight will appear as if they are in the main beam. This is known as an ambiguity error. Amplitude weighting of the array elements is used to reduce the side-lobes and hence to reduce this ambiguity. However, this will broaden the main beam and reduce directivity. **Note**: the energy must go somewhere.

Phased Array Pattern Synthesis

One of the major advantages of a phased array antenna is that the array excitation can be accurately controlled to produce any desired radiation pattern, potentially with extremely low side-lobes. Many methods have been developed to synthesise useful array factors. Here the Fourier transform method is introduced.

$$E(\theta) = \sum_{n=0}^{N-1} a_n \cdot \exp(-j\varphi_n) \cdot \exp\left(-j\left[\frac{2\pi}{\lambda} n d \sin(\theta)\right]\right) \quad \text{and} \quad v = \frac{d}{\lambda}\sin(\theta)$$

This is an equation of a a Discrete Fourier transform periodic in D with grating lobes every λ/D. The radiation pattern of the array is the Fourier transform of the complex element excitation. This method provides the least mean square approximation of the desired antenna pattern for $d = 0.5\lambda$.

Thus,

$$C_n = \frac{d}{\lambda} \int_{-\lambda/2d}^{\lambda/2d} E(\theta) \cdot \exp(-j2\pi n v) \cdot d\theta$$

Given a desired distribution pattern, $E(\theta)$, an expression for the complex weights may be obtained by orthogonality.

Aperture Efficiency

Aperture efficiency is a measure of maximum antenna directivity D_{max} and is defined as

$$D_{max} = \frac{P_{max}}{P_T/4\pi} = \frac{4\pi |E_{max}|^2}{P_T}$$

Where P_T is the total power supplied to the array and P_{max} is the power at the peak of the main

beam. From earlier we have

$$|E_{max}|^2 = \left| \sum_{n=0}^{N-1} a_n \right|^2$$

and

$P_T = \sum_{n=0}^{N-1} |a_n|^2$ where a_n is the weight applied to the field radiated by the n^{th} element

The aperture efficiency η is defined as D_w/D_u, where D_u is directivity of uniform illuminated aperture and D_w is directivity of weighted aperture of same size.

The aperture efficiency is

$\eta = \frac{|\sum a_n|^2}{N \sum |a_n|^2}$ summed over $n = 0 \rightarrow N-1$

Mutual Coupling

We recall that the purpose of an antenna is to efficiently couple a transmitter power inter free space. A mismatch will result in a standing wave one the feed line to the antenna. The voltage at the peak of this standing wave is $1 + |\Gamma|$ times greater than the voltage under matched conditions, where Γ is the voltage reflection coefficient. This corresponds to an increased power level that is $1 + |\Gamma|^2$ times greater than the incident power. Therefore the antenna radiates less power, and the individual components must be able to handle this power increase. This may also be a function of scan angle and can cause spurious lobes to appear in the far-field pattern. This is due to *mutual coupling*.

Consider a two element array with incident complex waves V_1 and V_2. Each element has reflected waves V_1' and V_2'. C_{11} is self coupling (as well as C_{22}), C_{12} is coupling between elements (as well as C_{21}).

$\Gamma_1 = \frac{V_1'}{V_1} = C_{11}\frac{V_1}{V_1} + C_{12}\frac{V_2}{V_1}$ (the same is true for Γ_2)

More generally for a linear array:

$$\boxed{\Gamma_{np} = \sum_{p,n=1}^{p,n} C_{np}\frac{V_p}{V_n}}$$

Various techniques have been postulated that aim to minimise Γ_{np} by multiplying by $[C_{np}]^{-1}$, i.e. nulling the mutual coupling. In large arrays this isn't a serious problem as the effects of the neighbouring elements cancel and tend to be uniform. However at the edges it does require some dummy elements terminated correctly to overcome problems at the array edge. This is a problem in small arrays (less than few tens of elements) as all elements act as edge elements (non-uniform coupling).

In some cases we observe that for certain directions close to those of grating lobes the active reflection coefficient becomes close to unity: almost all the transmitted power is reflected. This causes the appearance of a null in the radiation pattern and the array gain becomes zero in that direction. Several theories have been proposed to explain this phenomenon All concern the existence of surface waves whose coupling phenomena are the effects and whose propagation constant is precisely the coefficient.

Sub-arraying

Instead or as well as thinning the array, several elements may be grouped together and addressed with a single phase shifter. If we take the example of a 10 GHz array with dimensions 1m by 1m and group elements in units of 5 by 5, we then only have 200 groups requiring 200 phase shifters

and weighting calculators. This also has the effect of increasing the instantaneous band-width that can be handled by the antenna as the total time delay across the antenna is reduced.

Phased Array Errors

Temperature variations will change the shape and size of the antenna. This results in defocusing, reduced gain, increased side-lobes, beam-pointing errors and tracking errors. Some systems will use methods to counteract this (Invar rods), but these are expensive. Noise will impact on performance of phase shifters and combiners which again reduces system gain and increase side-lobes. Quantisation also reduces gain and increases side-lobes.

[maths omitted]

We observe that there is a reduction in peak gain. Energy conservation requires that the energy appear in the side-lobes. In radar systems that are power limited it is very important that these errors are kept to a minimum so that energy is used most efficiently.

Quantisation Side-lobes

In the case where all phase-shifters have the same phase origin, we get

$L = \frac{1}{2^p - 1}$

Also, the case where all the phase-shifters have a randomly-varying phase origin

$\bar{L} = \frac{\pi^2}{3N2^{2p}}$ or in dB $\bar{L}_{dB} = -10log_{10}N + 6p + 5$

The rms quantisation side-lobe level decreases by 6 dB for every additional bit and by 10 dB for each ten-fold increase in number of antenna elements.

Array Elements

The choice of array elements will depend on:

- Physical size
- Power handling
- Easy of manufacture / integration with existing array / cost
- Band-width
- Polarisation
- Gain / beam-width

Some example types:

- Wave-guide / slotted wave-guide
  - High power
  - Feed de-coupled from aperture
  - Large band-width
  - Element sizes are compatible with inter-element spacing (avoids grating lobes)
- Dipoles or Yagis
  - Either metal antennas or embedded radiators
  - Many potential designs
  - high powers

- Patch
  - Micro-strip feed lines
  - Low cost
  - Easy to fabricate
  - Narrow band
  - Low volume
- Notch
  - Printed circuit technology
  - Low cost
  - Potentially large band-width
  - Electronically small

Phase Shifters

Several different types

- Switched lines using PIN diodes, FETs or MEMS switches
  - Diodes used to switch in and out different path lengths
  - Switching speeds $< 1\mu s$, 3-6 bit accuacy, 0.5 dB per bit, few watts power handling
  - MEMS are slow with high isolation and low loss
- Vector modulators, at IF or RF
  - Acts as a complex attenuator: can steer anywhere in complex plane
  - Possibly a diode ring mixer or two double balanced mixers
- Ferrite phase shifter
  - Ferrite inserted into wave-guide
  - Phase controlled by current used to magnetise the ferrite
  - Switching $10 - 1000ms$, analogue or digital, insertion loss of 0.8-1.5 dB, high power handling
- Varactor phase shifter
  - Crude and not very repeatable
  - Pi-filter made from varactor (varicap) diodes and inductors. Capacitors controlled by DC voltage on control line. Varying voltage changes complex reactance of capacitors, and thus adjusts the relative phase.

TX/RX Modules

The T/R module integrates both of these functions into a small volume, light weight, low maintenance high duty cycle sub-system. The table below gives some performance parameters for specific models:

Freq Band	Power (W)	PE (%)	NF (dB)	Gain (dB)	Supplier
UHF	300-400	42	2.9	26-28	Raytheon

Freq Band	Power (W)	PE (%)	NF (dB)	Gain (dB)	Supplier
L	40-60	35-40	2.5-3.0	25-30	Raytheon
S	20-30	25-35	2.5-3.0	25-30	Raytheon
C	15-25	20-30	2.5-3.5	20-30	ITT
X	13-20	15-25	3.0-4.0	20-25	Raytheon

In quantity these T/R modules cost approximately $500 to $2000 each!

Feed Systems

Feed or power distribution systems for phased array antennas can take many forms and almost every radar system in production has a unique design or unique features. The essential features are:

- Low loss
- High amplitude and phase stability
- Accommodation of power distribution
- Flexibility
- Low cost
- Light weightings
- Small volume
- Wide band-width

Series Fed	Parallel Fed
Advantages Simple, low cost, flat profile strip-line/wave-guide, low loss.	**Advantages** Distributed power, good band-width, flexible, good aperture control.
Disadvantages Uniform power distribution, not flexible, limited band-width.	**Disadvantages** Heavy, bulky, expensive, higher losses.

Other feed types include:

Space Fed – The whole array is illuminated by the feed. Simple, low cost but inefficient, due to *spillover*. Difficult to control side-lobes.

Lens Fed – Similar to space fed except that an RF lens is used to deliver radiation to the aperture.

Reflect Array – This is similar to the lens fed concept except that the radiation is reflected from a short at the end of the phase-shifter.

Beam Steering

This consists of a computer to calculate the phase shift settings required for the phase shifters, the drivers to set the phase-shifters and data bus to send signals between the computer and drivers. For each phase shift, the computer has to recalculate everything and then re-set all the phase-shifters.

Phased Arrays in the Future

Phased arrays need to come down in cost; at the moment, the cost of a T/R module is too high. They hold the key to multi-function radar (MFR), an intelligent radar system able to optimise their own parameters in response to the observed environment. Plasma antennas potentially represent a future generation of low cost steerable antennas. Plasma is generated in a silicon substrate and shaped to create a mirror reflecting radiation causing a desired propagation pattern. All the antennas described here have been planar; many applications would benefit from antennas fitting a curved surface – so called *conformal* antennas. In military applications it is important that the phased array antenna does not increase the RCS of a platform carrying it, or even worse, give away and ID information.

Electronic Warfare

This is defined by the US Department of Defence as:

"Action involving the use of electromagnetic energy to determine, exploit, reduce or prevent hostile use of the electromagnetic spectrum, and action which retains friendly use of the electromagnetic spectrum".

In simple, the art (or science) of finding out about an enemy's forces, sensors and operations, by detecting and analysing the various signals that they emit, and attempting to confuse or deceive them by disrupting their operation and/or feeding them false information.

It is split into 3 sections: *electronic support* (ES), *electronic attack* (EA) and *electronic protection* (EP).

Electronic Support (ES)

Direction Finding

The direction of attack may be found by:

Mono-pulse (amplitude and phase comparison) between two beams.

Amplitude comparison in a set of beams.

Scanning a single beam continually in azimuth.

Other techniques such as super-resolution and DSP of signals arriving at the array.

We also care for the accuracy.

Amplitude Comparison in Mono-pulse

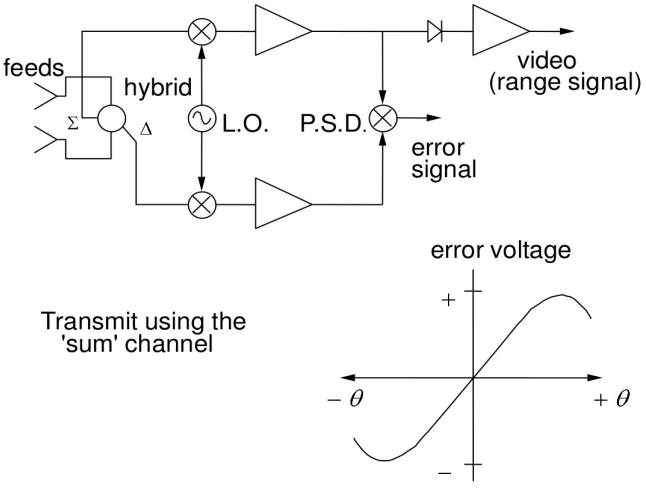

Super-Resolution

This relies on pushing the main lobe out of the 'real' domain and using the narrower back-lobe of the phased array.

Davies Beamformer

$\phi_1 = \frac{2\pi d}{\lambda}\sin(\theta_1)$ Where d is the inter-element spacing.

It allows us to put a null in the phased array antenna's far-field pattern.

The MUSIC Algorithm

Earliest and one of the best super-resolution. Not good for multi-path. Not mentioned here, yet. Too complex.

Frequency Measurement

Channelised receiver is good (Bragg cell). Scanning/swept receiver (spectrum analyser) not so good for short signals as the probability of intercept is low. Most common technique is instantaneous frequency measurement (IFM) – input signal split into two paths, one delayed, and then both rejoined at a digital phase discriminator. Phase difference at the output is $\omega\tau$ where τ is the time delay of the delayed path. This we can divide to get ω, the frequency. Can use a series of interferometers to overcome the IFM limitations in band-width.

Deinterleaving

Other parameters such as the pulse length can also be measured. Then is the task of sorting all the detected parameters out so that given emitters can be recognised. While the emitter can try to hide it's frequency, pulse lengths, etc, it cant change the direction of arrival.

Electronic Attach (EA)

Chaff

A cloud of metal strips which are ejected from aircraft or explosive charge. The strip length is $\lambda/2$, so that each strip acts as a resonant dipole, forming a large cloud of very high RCS, overloading the radar detection and track processor and masking true targets: Persistence of tens of minutes. A cloud of N dipoles scattered more than twice the wave-length apart has a radar cross section of $\sigma_n = 0.15N\lambda^2$

Noise Jamming

A jammer may be employed to protect the platform on which it is installed (self-screening jammer), to protect other platforms (mutual-screening) or from a safe distance to project other platforms closer to the threat radar (stand-off jammer). It may be a barrage jammer (covering a broad range of frequencies), a spot jammer (over a narrow band), a sweeping-CW, or gated. The important parameter is the jammer-to-signal ratio.

Self-Screening Jammer

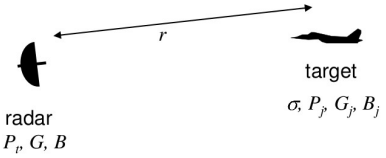

$$P_r = \frac{P_t G^2 \lambda^2 \sigma}{(4\pi)^3 r^4} \qquad P_{rj} = \frac{P_j G_j}{4\pi r^2} \frac{G\lambda^2}{4\pi} \frac{B}{B_j}$$

so :

$$\frac{P_{rj}}{P_r} = JSR = \left(\frac{P_j G_j G \lambda^2 B}{(4\pi)^2 r^2 B_j} \right) \Big/ \left(\frac{P_t G^2 \lambda^2 \sigma}{(4\pi)^3 r^4} \right) = \frac{P_j G_j B \, 4\pi r^2}{P_t G B_j \sigma}$$

i.e.

$$JSR = \frac{ERP_j}{ERP_r} \frac{B}{B_j} \frac{4\pi r^2}{\sigma} \frac{1}{N}$$

Stand-off Jammer

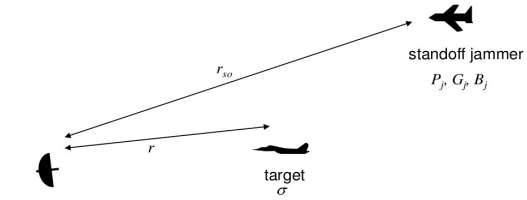

$$P_r = \frac{P_t G^2 \lambda^2 \sigma}{(4\pi)^3 r^4} \qquad P_{rj} = \frac{P_j G_j}{4\pi r_{so}^2} \frac{G_{SL} \lambda^2}{4\pi} \frac{B}{B_j}$$

so :

$$\frac{P_{rj}}{P_r} = JSR = \left(\frac{P_j G_j G_{SL} \lambda^2 B}{(4\pi)^2 r_{so}^2 B_j} \right) \Big/ \left(\frac{P_t G^2 \lambda^2 \sigma}{(4\pi)^3 r^4} \right) = \frac{P_j G_j G_{SL} B \, 4\pi r^4}{P_t G^2 B_j r_{so}^2 \sigma}$$

i.e.

$$JSR = \frac{ERP_j}{ERP_r} \frac{G_{SL}}{G} \frac{B}{B_j} \frac{4\pi r^4}{r_{so}^2 \sigma} \frac{1}{N}$$

Deception Jamming

The idea of jamming is to provide the victim radar with erroneous information, by generating signals that are similar to echoes that the radar expects but that contain false information or are higher than the ones of the real target. This can involve:

- Generating multiple false targets to confuse search radar.
- Range gate pull off against the tracking radar
- Velocity gate pull off
- Generation of targets with superimposed AM to generate false angular data in non-mono-pulse tracking radar.

Crosseye

The name given to a jamming technique to counter tracking systems. Two antennas are fed in anti-phase so that two contributions arrive at the victim radar $180°$ out of phase. Thus, the amplitude of the jammer goes through a zero at bore-sight. The wave-front of the jammer undergoes an abrupt discontinuity and the tracking radar will be thrown off track. It demands close tolerances to work correctly.

Electronic Protection (EP)

Low Probability of Intercept (LPI) Radar

We already noted that pulse compression is a useful EP technique since unless the jamming is matched to the pulse compression filter the radar receiver it will not benefit from the same processing gain as the wanted radar echoes. LPI radar carries this further by using pulse compression with a very high time-bandwidth product, hence allowing a relatively weak transmit power (a few watts). The pulse compression may be based on long chirp pulses and FM-CW operation. As the transmit power is low, it is not easy to detect by ES systems, hence the LPI.

Side-lobe Blanking

Here the radar antenna is provided with an auxiliary antenna whose radiation pattern is omni-directional and whose gain is just greater than the largest side-lobe (but less than the main beam). If the signal on the auxiliary antenna is larger than the main signal, the target is blanked, as it must have come from a side-lobe.

Side-lobe Cancellation

The radiation pattern on receive of a radar can be modified adaptively to suppress jamming received via the side-lobes. This technique is called *sidelobe cancellation*. It uses one or more auxiliary antenna elements, whose signals are weighted in amplitude and phase before being combined with the signal from the primary antenna. The weights applied to the auxiliary element signals are derived from adaptive cancellation loops.

Adaptive Arrays

Whilst a side-lobe canceller can suppress jamming received via the side-lobes of the primary antenna, it cannot do anything about main beam jamming. However, a phased array radar with signals digitised at each element (or sub-array) can allow an optimum radiation pattern to be formed on receive, with a maximum in the a desired direction of look, whilst at the same time suppressing jamming received from any other directions.

The Optimum Array

We chose to maximise the ratio between gain in a given direction and total noise power.

$$D_0 = \begin{bmatrix} 1 \\ \exp(j2\pi\tau_0) \\ \vdots \\ \exp(j2\pi N\tau_0) \end{bmatrix}$$

$\hat{\mathbf{W}} = k\mathbf{R}^{-1}\mathbf{D}_0$ where k is a scalar constant

Stealth & Counter Stealth

This section looks at the techniques used to reduce the radar signature of a target, the reduction of target detection performance that gives, and some of the radar techniques that might be used to recover the advantage that the reduced RCS has bought.

Stealth Techniques

There are several techniques that are used to reduce the radar signature of a target:

- Cover the surface with Radio Absorbing Material (RAM).
- Use RF-transparent composite materials
- Shape the target to reduce edges, surface discontinuities and corners (right angles).
- Shape the target to reflect radiation in directions other than in the source direction.

The ability to calculate the RCS of a target of a known size and shape is clearly central to the ability to reduce the target's radar signature. This requires huge computing power and good EM models. Aircraft designed to have a low RCS are not aerodynamically steady – sophisticated control systems actively maintain the aircraft in flight.

Radio Absorbing Materials (RAM)

Essentially a matter of designing materials to present a particular impedance to an incident electromagnetic wave. The Fresnel equations for the reflection coefficients at the boundary between free space and a semi-infinite medium are used. They are functions of the incident angle, polarisation, and material properties (μ_r and ε_r).

Sailsbury Screen

One of the oldest types of absorber consists of a resistive sheet spaced in front of a metal sheet by a low dielectric material (plastic foam or honeycomb). For zero reflectivity, a sheet of $377\Omega/sq$ (size not important, just as long as the area is square). This is matched to a specific frequency due to the spacing between the honeycomb and metal sheet being a $\lambda/4$.

The Jaumann absorber gives an improved band-width on the Sailsbury Screen by adding multiple screens and spacers.

Contrail Suppression

Contrails (white trails behind aircraft) may be suppressed by injecting chlro-fluro sulphuric acid into the engine exhaust gasses. This reduces the size of the water particles so they scatter less light.

Sensor Signatures

We need to be careful that we don't have a stealth aircraft to radar, but our own radar and communications systems transmit enough information to give us away. There's no point in having a stealth platform if our own sensors become the main RCS signature dominators.

$\sigma_A = \frac{G^2\lambda^2|\rho|^2}{4\pi}$ Where ρ is the voltage reflection coefficient.

Whilst this may be low within the radar's operating range, it may be very high outside. The antenna's operational termination may cause scattering too. This leads to the concept of the *minimum scattering antenna*.

Measurement of Target Signature

This is extremely important not only in design but in operation too – a small amount of damage may cause a massive change in RCS. Signatures are measured on special ranges; models may be used during design. One important technique is ISAR, in which we rotate our target in front of a radar to allow for high resolution imaging of the RCS, allowing hot-spots to be identified.

Counter Stealth

There are several radar techniques to overcome (or to attempt to overcome) the advantages that come from counter-stealth.

- Bistatic Radar – stealth RCS reduction aims to reduce mono-static radar. Energy scattered away from the mono-static radar may be collected by a bistatic radar.
- Low frequency (HF or VHF) radar – the target signature is increased at frequencies at which the target dimensions are resonant; if you can make the RF resonate around the aircraft the RCS will be large. RAM is also less efficient at low frequencies.
- Ultra-wideband (UWB) radar – this may exploit any target resonances (mentioned for low frequency). It is very difficult to make a target stealthy over a large band-width.
- Networked radars
- Factors to improve performance in traditional radar, counteracting the loss due to reduced RCS: improved clutter models, reduced phase noise and improved tracking algorithms, as well as the flexibility of phased array antennas to give longer dwell times.

Bistatic Radar

The next section describes this in more detail.

- RCS reduction techniques aimed at minimising mono-static RCS; bistatic geometry is different, and the stealth may not reduce bistatic RCS.
- Forward scatter geometry can give a high RCS even for truly stealthy targets.
- Passive receiver, immune to interception – utilises 'illuminators of opportunity'.

Low Frequency Radar

Issues with resolution, both in azimuth (antenna size) and range (band-width). Also with interference from other users of these frequencies. Note also FOPEN properties of low frequency.

Ultra-wideband Radar

Can be defined as a radar with a fractional band-width greater than 0.25. UWB radar systems in two basic types:

- *Impulse Radars* transmit a very narrow, high power impulse and process the received echo in the time domain. The hardware is rather specialist, especially for anything but short range. High power and high instantaneous band-width required.
- The second type uses pulse compression principles to obtain high range resolution typically with wideband chirp or step-CW wave-forms. The peak power requirements are much lower, and the hardware doesn't necessarily have to support the same instantaneous band-width.

Note also that there are spectral interpolation techniques, in which data from different bands of radar can be bought together.

Bistatic Radar

Basic Definitions

- Monostatic radar: TX and RX at the same location (or near enough).
- Bistatic radar: TX and RX separated by a considerable distance to achieve a benefit (technical, operational or cost).
- Radar net: Several radars linked together to improve coverage or accuracy.
- Multiliteration radar: Radar net using range-only data.
- Multistatic radar: Bistatic radar net with multiple TX and/or RX.
- Hitchhiker: Bistatic RX operating with the TX of a monostatic radar.
- Passive Bistatic: Bistatic RX with other TX of opportunity (eg broadcast radio TX).

Introduction

Bistatic radar has many potential advantages in detection of stealthy targets which are shaped to scatter energy in directions away from the monostatic source radar. The receiver is covert and therefore safer in many situations. Countermeasures are difficult to deploy against bistatic radar. Increasing use of UAV makes bistatic radar attractive. Many of the synchronisation and geolocation issues are now readily soluble using GPS. The extra degrees of freedom may make it easier to extract information from bistatic radar clutter for remote sensing.

Geometry

The baseline, L, is the distance between the TX and the RX. θ_R is the angle between the normal to the ground at the RX and target, which is distance R_R from the receiver. θ_T gives the angle between the normal to the ground at the TX and the target, at a range of R_T. $\beta = \theta_T - \theta_R$. β is the angle at the target.

$R_R = \frac{(R_T+R_R)^2-L^2}{2(R_T+R_R+L\sin(\theta_R))}$

$R_T + R_R = constant$

Targets lying on the TX-RX baseline have a zero bistatic range.

Doppler

For $V_T = V_R = 0$, and $V \neq 0$. δ is the angle between the L baseline and the target velocity, V.

$f_D = \frac{2V}{\lambda} \cdot \cos(\delta) \cdot \cos\left(\frac{\beta}{2}\right)$

Special cases exist. If $\beta = 0°$, the system is monostatic. If $\beta = 180°$, the system is working with forward scatter.

Bistatic Properties

We will look at the bistatic radar equation, bistatic RCS, forward scatter, bistatic clutter, bistatic ambiguity functions and pulse chasing.

Bistatic Radar Equation

This is derived in the same way as with monostatic radar. $\frac{P_R}{P_N} = \frac{P_T G_T G_R \lambda^2 \sigma_b L_p}{(4\pi)^3 R_T^2 R_R^2 k T_0 B F}$

We should also add pattern propagation factors in for the TX-target (F_T) and target-RX (F_R) paths.

$\frac{P_R}{P_N} = \frac{P_T G_T G_R F_T^2 F_R^2 \lambda^2 \sigma_b L_p}{(4\pi)^3 R_T^2 R_R^2 k T_0 B F}$

The maximum signal-to-noise radio is obtained when $R_T = R_R$. It is highest for targets close to the TX or the RX.

Bistatic RCS

Bistatic RCS is equal to the mono-static RCS at the bisector of the bistatic angle, β, reduced in frequency by the factor $\cos(\beta/2)$ given:

- Sufficiently smooth targets
- No shadowing
- Retro-reflectors persistence

Three bistatic RCS phenomena that may be exploited as counter-stealth are:

- Resonance scatter
- Forward scatterers
- Specular reflection

Resonance Scatter

Well documented for mono-static radar. Explained by interference between the incident wave and the creeping wave, which circles the target. The effect is that when these sum up for various parts of the aircraft (wing, fuselage, tail, inlet, exhaust, etc) the resulting resonance significantly enhances the RCS. For a aircraft, this seems to happen at about 270 MHz, based on computer models of wire-frame aircraft.

Forward Scatter

Babinet's principle tells us that we get exactly the same scattering from a perfectly absorbing target as we would get from a target-shaped hole in an infinite perfectly conducting sheet.

So a target on the TX-RX baseline, even if completely stealthy, will scatter an significant amount of energy: the RCS will be of the order

$\sigma_b = \frac{4\pi A^2}{\lambda^2}$

with an angular scattering of λ/d radians, which tends to favour low frequencies. Targets lying on the baseline will have no range and no Doppler information – forward scatter is good for detection but poor for location and tracking.

Specular Reflection

The ability to detect specular reflections which have been specifically deflected away from the mono-static source. To catch a target by this method would work only for specific geometries, and only for very short durations – the change of detecting the target in this scenario is optimistic at best.

Bistatic Clutter

Bistatic clutter is basically all of the problems suffered by mono-static clutter, plus geometry. Little data exists yet.

Bistatic Ambiguity

Expresses a point target response as a wave-forms as a function of delay and Doppler frequency, or range and velocity.

$$|\chi(\tau, v)|^2 = \left| \int u(t) \cdot u^*(t+\tau) \cdot \exp(j2\pi vt) \cdot dt \right|^2$$

Bistatic geometry can have an effect on the bistatic ambiguity since relationships are non-linear.

Pulse Chasing

If a transmitter scans in azimuth, and if the receiver uses a directional antenna, then the direction in which the receive beam must be pointing is a very non-linear function of time. This means that the receiver must use either a fan or mixed beams or a scanned beam which (since the system is non-linear) must be electronically scanned.

Beam scan rate:

$\dot{\theta}_R = \frac{c \tan(\beta/2)}{R_R}$

Passive Bistatic Radar (PBR)

In general, bistatic radar systems use dedicated transmitters with explicit control over location, scan pattern, etc. However, it is possible to use transmissions that just happen to be there – these are known as illuminators of opportunity. Such transmissions may be other radars, communications broadcast or navigation signals. In these days of spectral congestion, there are more and more sources to choose from – they are often high power and favourably sited. They also use parts of the spectrum that are not usually available for radar use. As well as that, no license to transmit is required. The radar is covert, so countermeasures are difficult to deploy.

Coverage Prediction

Maximum integration dwell time is approximately

$T_{max} = \sqrt{\frac{\lambda}{A_R}}$

Target Location and Tracking

Bistatic systems can measure:

- Bistatic range
- Echo Doppler
- Echo angle of arrival

They can be combined using:

- Multilateration
- Parameter estimation

Sonar

Did not have time to include this...

Note, speed of sound:

In Air:	340.29 m/s	(at sea level)
In Water:	1,484 m/s	(4.3× that of air)

Sources

This document is based on MSc Lecture Notes in "*Radar Systems*" from Prof. Hugh Griffiths, E&EE, UCL.

Those notes are, in turn, based on the book "An Introduction to Radar Systems" by Merrill Skolnik.

Disclaimer

Note

This document was written by:

George Smart

Undergraduate Student, MEng.

Department of Electronic & Electrical Engineering

University College London

Website: http://www.george-smart.co.uk/

Date: February 2011

LaTeX

```
\boxed{|\chi(\tau, v)|^2 = \left | \int u(t) \cdot u^*(t+\tau) \cdot \exp(j 2 \pi v t) \cdot dt\right |^2}

\frac{P_R}{P_N} = \frac{P_T G_T G_R F_T^2 F_R^2 \lambda^2 \sigma_b L_p}{(4 \pi)^3 R_T^2 R_R^2 k T_0 B F}

\frac{P_R}{P_N} = \frac{P_T G_T G_R \lambda^2 \sigma_b L_p}{(4 \pi)^3 R_T^2 R_R^2 k T_0 B F}

f_D = \frac{2V}{\lambda} \cdot \cos(\delta) \cdot \cos \left (\frac{\beta}{2} \right )

R_R = \frac{(R_T + R_R)^2 - L^2}{2(R_T + R_R + L\sin(\theta_R))}

\boxed{\Gamma_{np} = \sum\limits_{p,n=1}^{p,n} C_{np} \frac{V_p}{V_n}}

\left | E_{max} \right|^2 = \left | \sum\limits_{n=0}^{N-1} a_n \right |^2

E(\theta) = \sum\limits_{n=0}^{N-1} a_n \cdot \exp(-j \varphi_n) \cdot \exp \left ( -j \left [\frac{2 \pi}{\lambda} nd \sin (\theta) \right ] \right )

N \pi \frac{d}{\lambda} \left [ \sin \left ( \theta_0 + \frac{\theta_{3dB}}{2} \right ) - \sin(\theta_0) \right ] = \frac{\pi}{2}

\boxed{\frac{\sin \left [ N \left ( \frac{\pi d \sin(\theta)}{\lambda} - \frac{\varphi}{2} \right ) \right ]}{N \sin \left ( \frac{\pi d \sin(\theta)}{\lambda} - \frac{\varphi}{2} \right )}}

\sum\limits_{n=0}^{N-1} x^n = \frac{x^N – 1}{x – 1} = x^{N-1/2} \frac{x^{N/2} – x^{-N/2}}{x^{1/2}-x^{-1/2}}

\sum\limits_{n=0}^{N-1} \exp \left ( j n\left ( \frac{2 \pi}{\lambda} d \sin(\theta) - \varphi \right ) \right )

F(\sin(\theta)) = \sum\limits_{n=0}^{N-1} a_n \cdot f(\sin(\theta)) \cdot e^{j \frac{2 \pi}{\lambda} nd \sin(\theta)}

\boxed{P_r = \frac{2.3\times10^{-11} P_t G_t G_r Z \Delta\theta \Delta\phi L_{sys} L_{atmos}}{\lambda^2 R^2}}

\boxed{\sigma_{scatt} = \frac{C \pi^5}{\lambda^4}\sum\limits_{i=1}^{N} D^6_i \; \; \; [m^2]}
```

```
\left[ \begin{array}{ccc}
E^s_v \\
E^s_h \\
\end{array} \right] = \left[ \begin{array}{ccc}

S_{vv} & S_{vh} \\
S_{hv} & S_{hh} \\
\end{array} \right] = \left[ \begin{array}{ccc}

E^i_v \\
E^i_h \\
\end{array} \right]
```

$$\boxed{\theta = \cos^{-1} \left(\frac{r_2^2 - r_1^2 - B^2}{2B r_1} \right) - \alpha}$$

$$\boxed{P_r = \frac{P_t G^2 \lambda^2 \sigma^0 ct \Theta_B}{(4 \pi)^3 r^3 2 \sin(\alpha)}}$$

$$\boxed{\Delta x = \frac{r_0 \lambda}{2v} \cdot \frac{vd}{r_0 \lambda} = \frac{d}{2}}$$

$$\boxed{f_D = \frac{2r}{c} \cdot \frac{\Delta f}{\Delta t} = \frac{2 \Delta f}{c \Delta t} \cdot r}$$

$$\boxed{u(t) = A(t) \cdot \cos \left (2 \pi f_0 t + \frac{\pi B t^2}{T} + \frac{2 \pi B^2 t^3}{3 f_0 T^2} \right)}$$

$$\boxed{\frac{1}{2 \pi} \frac{d}{dt} \left [\frac{2 \pi f_0^2 T}{B} \ln \left (1 - \frac{B t}{f_0 T} \right) \right] = \frac{2 \pi f_0^2 T}{f_0 T - Bt}}$$

$$\boxed{u(t) = A(t) \cdot \cos \left [\frac{2 \pi f_0^2 T}{B}\ln \left (1- \frac{B t}{f_0 T}\right)\right]}$$

$$\boxed{X(t, \omega_D) = \int\limits_{-\infty}^{\infty} u(t) u^*(T-t) e^{j \omega_D t}dt}$$

$$\boxed{\big |\chi(\tau, v) \big |^2 = \left | \int u(t) u^*(t+\tau) e^{j2\pi vt}dt \right |^2}$$

$$\boxed{\mu = \frac{2 \pi B}{T}}$$

$$\boxed{u(t) = \cos \left (\omega_0 t + \frac{\mu t^2}{2} \right)}$$

$$\boxed{H(\omega) = K F^* (\omega) e^{-j \omega t_0}}$$

$$\boxed{\frac{P_r}{P_n} = \frac{P_t \tau G^2 \lambda^2 \sigma L}{(4 \pi)^3 r^4 k T_0 F}}$$

$$\boxed{\hat{R} = \frac{1}{K}\sum\limits_{k=1}^K Y_k Y_k^H}$$

$$\boxed{f_D = \frac{2 v f_0 \sin (\theta)}{c}}$$

$$\boxed{\hat{\mathbf{W}}=k \mathbf{C}^{-1}\mathbf{D_0}}$$

$$\boxed{I = \frac{\bar{S_o}/C_o}{\bar{S_i}/C_i} = \frac{\bar{S_o}}{\bar{S_i}} \cdot CA}$$

$$\boxed{CA = \frac{input\; clutter}{output\; clutter} = \frac{C_i}{C_o}}$$

$$\boxed{\left | H(\omega) \right | = \left (2 \left | \sin \left (\frac{\omega T}{2} \right) \right | \right)^2 = 4 \left | \sin^2 \left (\frac{\omega T}{2} \right) \right |}$$

$$\boxed{v_{blind} = \frac{n \cdot \frac{\lambda}{2}}{PRI} = \frac{n \cdot c \cdot PRF}{2 f_0}}$$

$$\boxed{\left | H(\omega) \right | = 2 \left | \sin \left (\frac{\omega T}{2} \right) \right |}$$

$$\boxed{f_D = - \frac{1}{2 \pi} \frac{d}{d t}\left (\frac{4 \pi r}{\lambda} \right) = -\frac{2}{\lambda}\frac{dr}{dt} = - \frac{2vf_0}{c}}$$

$$\boxed{f_D = - \frac{1}{2 \pi} \frac{d \phi}{d t}}$$

$$\boxed{\phi = 2 \pi \frac{2r}{\lambda}}$$

$$\boxed{\frac{A}{\Psi_0} = \frac{signal\; amplitude}{rms\; noise\; voltage} = \sqrt{\frac{2S}{N}}}$$

$$\boxed{P_{d} = \int\limits_{V_T}^{\infty}p_s(R)_{target+noise} \cdot dR}$$

$$\boxed{P_{FA} = \int\limits_{V_T}^{\infty}p_n(R)_{noise \; alone} \cdot dR}$$

$$\boxed{P_r = \frac{P_t G_0^2 \lambda^2 \sigma \cdot cosec(\theta)}{(4 \pi)^3 r^4}}$$

$$\boxed{G = G_0 \cdot \frac{r^2}{h^2} = G_0 \cosec^2(\theta)}$$

$$\boxed{P_r = \frac{P_t G^2 \lambda^2 \sigma}{(4 \pi)^3 r^4}}$$

$$\boxed{\frac{P_r}{P_n} = \frac{P_m}{\tau \cdot PRF} \cdot \frac{4 \pi}{\omega} \cdot \frac{4 \pi A_e}{\lambda^2} \cdot \frac{\lambda^2 \sigma L}{(4 \pi)^3 r^4 k T_0 B F} \cdot T_d \cdot \frac{\omega}{\Omega} \cdot PRF}$$

$$\boxed{T_b = T_d \cdot \frac{\omega}{\Omega}}$$

$$\boxed{\sigma = \frac{n^2 G_e^2 \lambda^2}{4 \pi}}$$

$$\boxed{\sigma = \frac{4 \pi A^2}{\lambda^2}}$$

$$\boxed{r_{max} = \sqrt[4]{\frac{P_t G^2 \lambda^2 \sigma L}{(4 \pi)^3 k T_0 B F (SNR)}}}$$

STANDARD RADAR EQUATION

$$\boxed{SNR = \frac{P_r}{P_n} = \frac{P_t G^2 \lambda^2 \sigma L}{(4 \pi)^3 r^4 k T_0 B F}}$$

$$\boxed{P_n = k T_0 B F}$$

$$\boxed{P_r = \frac{P_t G}{4 \pi r^2} \cdot \sigma \cdot \frac{1}{4 \pi r^2} \cdot \frac{G \lambda^2 }{4 \pi}}$$

$$\boxed{A_e = \frac{G \lambda^2 }{4 \pi}}$$

$$\boxed{Pd = \frac{P_t G}{4 \pi r^2} \cdot \sigma \cdot \frac{1}{4 \pi r^2} \cdot A_e}$$

$$\boxed{Pd = \frac{P_t G}{4 \pi r^2} \cdot \sigma \cdot \frac{1}{4 \pi r^2}}$$

$$\boxed{P_r = \frac{P_t G}{4 \pi r^2} \cdot \sigma}$$

$$\boxed{Pd = \frac{P_t G}{4 \pi r^2}}$$

$$\boxed{Pd = P_t \cdot \frac{1}{4 \pi r^2}}$$

$$\boxed{N_{pulses} = T \cdot \frac{\Theta_B}{360^\circ} \cdot PRF}$$